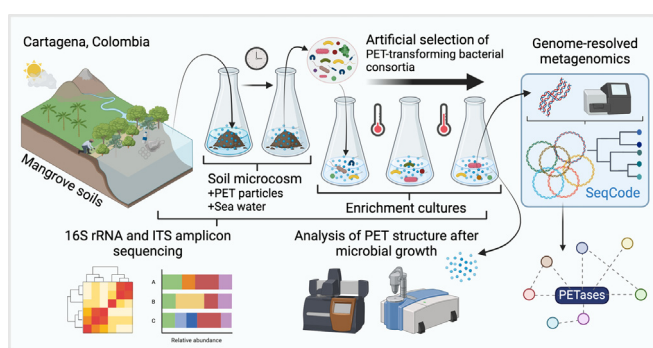


Research Article

Engineering the mangrove soil microbiome for selection of polyethylene terephthalate-transforming bacterial consortia



Engineering microbiomes to effectively transform plastics is an exciting research theme in microbiology and biotechnology. Here, we developed and implemented an approach to artificially select polyethylene terephthalate (PET)-transforming bacterial consortia using mangrove soils. Our results enhanced the ecological understanding of PET transformation and described putative novel PET-degrading enzymes obtained via genome-resolved metagenomics.

Jimenez Diego Javier Jiménez, Dayanne Chaparro, Felipe Sierra, Gordon F. Custer, Golo Feuerriegel, Maria Chuvochina, Laura Diaz-Garcia, Lucas William Mendes, Yina Paola Ortega Santiago, Carolina Rubiano-Labrador, Felipe Salcedo Galan, Wolfgang R. Streit, Francisco Dini-Andreote, Alejandro Reyes, Alexandre Soares Rosado

diego.jimenezavella@kaust.edu.sa

(D.J. Jiménez)

alexandre.rosado@kaust.edu.sa

(A.S. Rosado).

Highlights

Flooding with seawater and intrusion of polyethylene terephthalate (PET) particles have reshaped the mangrove soil microbiome.

We developed and implemented an approach to select bacterial consortia involved in PET transformation.

The obtained consortia mainly comprised *Pseudoxanthomonas winnipegensis*, *Brevibacillus* spp., and *Mangrovimarina plasticivorans* gen. nov. sp. nov.

Putative novel PET-degrading enzymes were detected via genome-resolved metagenomics.

Evidence suggested that the catabolism of PET-derived monomers occurs via co-metabolism across distinct taxa in the consortia.
















Trends in Biotechnology, Month 2024,

Vol. xx, No. xx

<https://doi.org/10.1016/j.tibtech.2024.08.013>

Research Article

Engineering the mangrove soil microbiome for selection of polyethylene terephthalate-transforming bacterial consortia

Diego Javier Jiménez ^{1,13,14,*,@}, Dayanne Chaparro ^{2,3}, Felipe Sierra ^{2,3}, Gordon F. Custer ^{4,5}, Golo Feuerriegel ⁶, Maria Chuvochina ⁷, Laura Diaz-Garcia ⁸, Lucas William Mendes ⁹, Yina Paola Ortega Santiago ^{10,11}, Carolina Rubiano-Labrador ¹², Felipe Salcedo Galan ¹⁰, Wolfgang R. Streit ⁶, Francisco Dini-Andreote ^{4,5}, Alejandro Reyes ³, and Alexandre Soares Rosado ^{1,13,*}

Mangroves are impacted by multiple environmental stressors, including sea level rise, erosion, and plastic pollution. Thus, mangrove soil may be an excellent source of as yet unknown plastic-transforming microorganisms. Here, we assess the impact of polyethylene terephthalate (PET) particles and seawater intrusion on the mangrove soil microbiome and report an enrichment culture experiment to artificially select PET-transforming microbial consortia. The analysis of metagenome-assembled genomes of two bacterial consortia revealed that PET catabolism can be performed by multiple taxa, of which particular species harbored putative novel PET-active hydrolases. A key member of these consortia (*Mangrovimarina plasticivorans* gen. nov., sp. nov.) was found to contain two genes encoding monohydroxyethyl terephthalate hydrolases. This study provides insights into the development of strategies for harnessing soil microbiomes, thereby advancing our understanding of the ecology and enzymology involved in microbial-mediated PET transformations in marine-associated systems.

Introduction

Mangrove ecosystems are biodiversity hotspots that support several ecosystem services, such as erosion control, protection against storms, and intertidal zone buffering. Mangrove soils serve as reservoirs of sequestered atmospheric carbon, and their associated microbiomes are essential for the biochemical cycling of nutrients [1–3]. These dynamic habitats harbor myriad life forms and are subject to a near-constant input of microbial communities, nutrients, and plastics from the ocean, which directly can affect their functionality [4]. Despite their importance, mangroves are threatened worldwide by multiple anthropogenic stressors and global change factors, including pollution (e.g., oil and plastics), deforestation, land-use change, erosion, nutrient runoff, sea-level rises, and shifts in temperature and salinity [3,5,6]. Mangrove soils in tropical and subtropical areas also act as sinks of various fossil fuel-based microplastics (e.g., polyolefins and polyesters) [7–9]. These plastic particles influence the ecological properties of mangrove soils by increasing carbon availability, affecting water evaporation, altering the physical structure of the soil environment, releasing toxic compounds, and serving as vectors for microbial dispersal [10–12]. Given that mangroves are constantly exposed to human activities, plant-derived polymers, and plastic pollution, mangrove soils have been highlighted as a potential source of alpha/beta-fold hydrolases and plastic-active microorganisms [13–16]. However, the effects of microplastic pollution on microbial diversity and metabolic activities in mangrove soils remain

Technology readiness

Engineering microbiomes to transform plastics is a daunting task. Here, we reported the development and implementation of a strategy to select polyethylene terephthalate (PET)-transforming microbial consortia from mangrove soils. The approach can be broadly applicable using microbial inocula from divergent terrestrial and aquatic systems. Details on the concepts and fundamentals explored in this study are reported in previous studies. However, our work reports laboratory-scale findings, which require optimization and scalability for potential use at industrial settings. Thus, most of these results and findings must be translated into future research and development. In addition, we advocate the use of techniques able to provide fine-scale resolution and quantification of PET degradation in experimental assays. Finally, advances in microbial culturing techniques targeting the isolation of members of PET-transforming consortia can allow the design of minimal synthetic consortia for production and implementation in biotechnological processes. Within NASA's Technology Readiness Level (TRL) system, we propose that our strategy has reached TRL2.

¹Biological and Environmental Sciences and Engineering Division (BESE), King Abdullah University of Science and Technology (KAUST), Thuwal, Kingdom of Saudi Arabia

²Microbiomes and Bioenergy Research Group, Department of Biological Sciences, Universidad de los Andes, Bogotá, Colombia

underexplored [17]. Considering the inherent complexity of these ecosystems and challenges of *in situ* experimental studies, controllable and reproducible systems (e.g., microcosms) could be used to investigate the effects of multiple environmental factors (e.g., flooding, drought, and salinity) on the mangrove soil plastisphere (defined as the soil microbiota under the direct influence of plastic particles). This may enable a better understanding of how microbes deal with microplastic pollution in a dynamic and changing ecosystem [18–21].

PET is one of the most abundant thermoplastic polyesters found in mangrove soils and surface seawater [9]. Recent evidence revealed that specific microbes decompose PET through a series of catabolic reactions despite being highly recalcitrant, with an estimated half-life of ~2.3 years in a marine environment [22]. This is a two-step process involving: (i) depolymerization, which is catalyzed by PET hydrolase (PETase) and monohydroxyethyl terephthalate (MHET) hydrolase (MHETase); and (ii) intracellular assimilation of PET-derived monomers [i.e., terephthalic acid (TPA) and ethylene glycol (EG)]; this process has been well described in the bacterium *Ideonella sakaiensis* [23]. Recent efforts to identify and mine PET-depolymerizing enzymes in natural environments have yielded novel PETases derived from bacterial phyla, such as *Pseudomonadota*, *Actinomycetota*, *Bacteroidota*, and *Bacillota* [24–26]. Although specific PET-degrading enzymes have been characterized and subsequently engineered to enhance their catalytic activity in bio-upcycling processes [27–29], information regarding the eco-enzymology (i.e., the study of enzymes and their role in microbial interactions and the modification of surrounding environments) and catabolism of PET by soil-derived microbial communities remains limited. Therefore, simplified synthetic bacterial consortia have been designed to improve the transformation of PET and its derived chemical compounds in experimental settings [30–33]. Unfortunately, these studies did not fully capture the complexity and functional diversity of microorganisms commonly found in soil; however, this can be achieved via soil microbiome engineering by using top-down strategies to artificially select PET-transforming microbial consortia [34].

A recent study combined soil microcosms amended with plastics, followed by subsequent liquid enrichment culture to improve the selection of polyethylene (PE)-degrading microbial consortia [35]. Furthermore, a long-term enrichment system (~2 years) was required to effectively isolate PET-degrading bacteria from deep sea sediments [36]. In general, top-down strategies comprise three interlinked processes: (i) enrichment; (ii) artificial selection; and (iii) directed evolution [37]. During the enrichment process, natural communities are forced to survive under specific culture conditions (e.g., using a sole carbon source), allowing the progressive selection of the fittest species. In this process, a rational modification of culture conditions may optimize the selection of communities with the desired functions [38,39]. This enrichment process is common for the selection of plant biomass-degrading microbial communities [40,41]. Next, during artificial selection and directed evolution processes, the best-performing microbial communities are used as seeds to start a new growth cycle that generates offspring consortia with enhanced performance [34,37,42].

This study combined a microcosm experiment with a top-down strategy to evaluate the impact of PET particles on the mangrove soil microbiome in the presence or absence of seawater and to select PET-transforming microbial consortia using an enrichment culture experiment. Our findings provide new insights for an improved understanding of the mangrove soil plastisphere under distinct environmental scenarios. Additionally, we report the development of PET-transforming bacterial consortia using an artificial selection approach, which resulted in the identification of putative novel PET-depolymerizing enzymes and two novel bacterial taxa. Finally, we provide genomic evidence for a cooperative/labor division strategy of taxa enriched in the bacterial consortia, which has direct implications for PET transformations.

³Max Planck Tandem Group in Computational Biology, Department of Biological Sciences, Universidad de los Andes, Bogotá, Colombia

⁴Department of Plant Science and Huck Institutes of the Life Sciences, The Pennsylvania State University, University Park, PA, USA

⁵The One Health Microbiome Center, Huck Institutes of the Life Sciences, The Pennsylvania State University, University Park, PA, USA

⁶Department of Microbiology and Biotechnology, University of Hamburg, Hamburg, Germany

⁷The University of Queensland, School of Chemistry and Molecular Biosciences, Australian Centre for Ecogenomics, Brisbane, Queensland, Australia

⁸Department of Chemical and Biological Engineering, Advanced Biomanufacturing Centre, University of Sheffield, Sheffield, UK

⁹Cell and Molecular Biology Laboratory, Center for Nuclear Energy in Agriculture, University of Sao Paulo, Piracicaba, SP, Brazil

¹⁰Department of Chemical and Food Engineering, Universidad de los Andes, Bogotá, Colombia

¹¹Research Management, Agroindustrial Production and Transformation Research Group (GIPTA), Department of Agroindustrial Sciences, Universidad Popular del Cesar, Aguachica, Cesar, Colombia

¹²Chemical and Biological Studies Group, Basic Sciences Faculty, Universidad Tecnológica de Bolívar, Cartagena de Indias, Colombia

¹³Web address: <https://megb.kaust.edu.sa/people>

¹⁴Lead contact.

*Correspondence: diego.jimenezavella@kaust.edu.sa (D.J. Jiménez) and alexandre.rosado@kaust.edu.sa (A.S. Rosado).

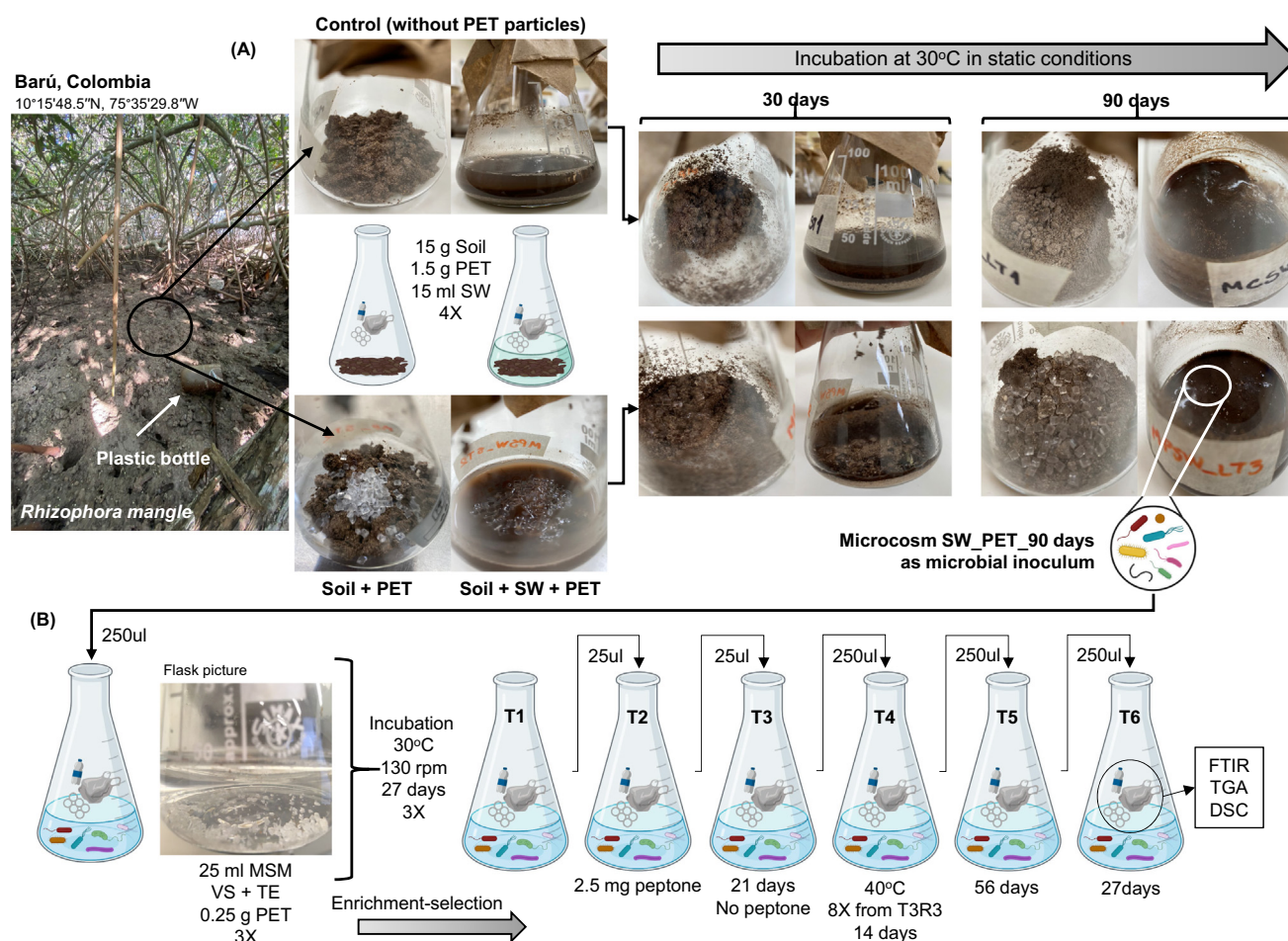
✉X: @Jimenez_ADJ (D.J. Jiménez).

Results and discussion

Effects of multiple factors on the mangrove soil microbiome

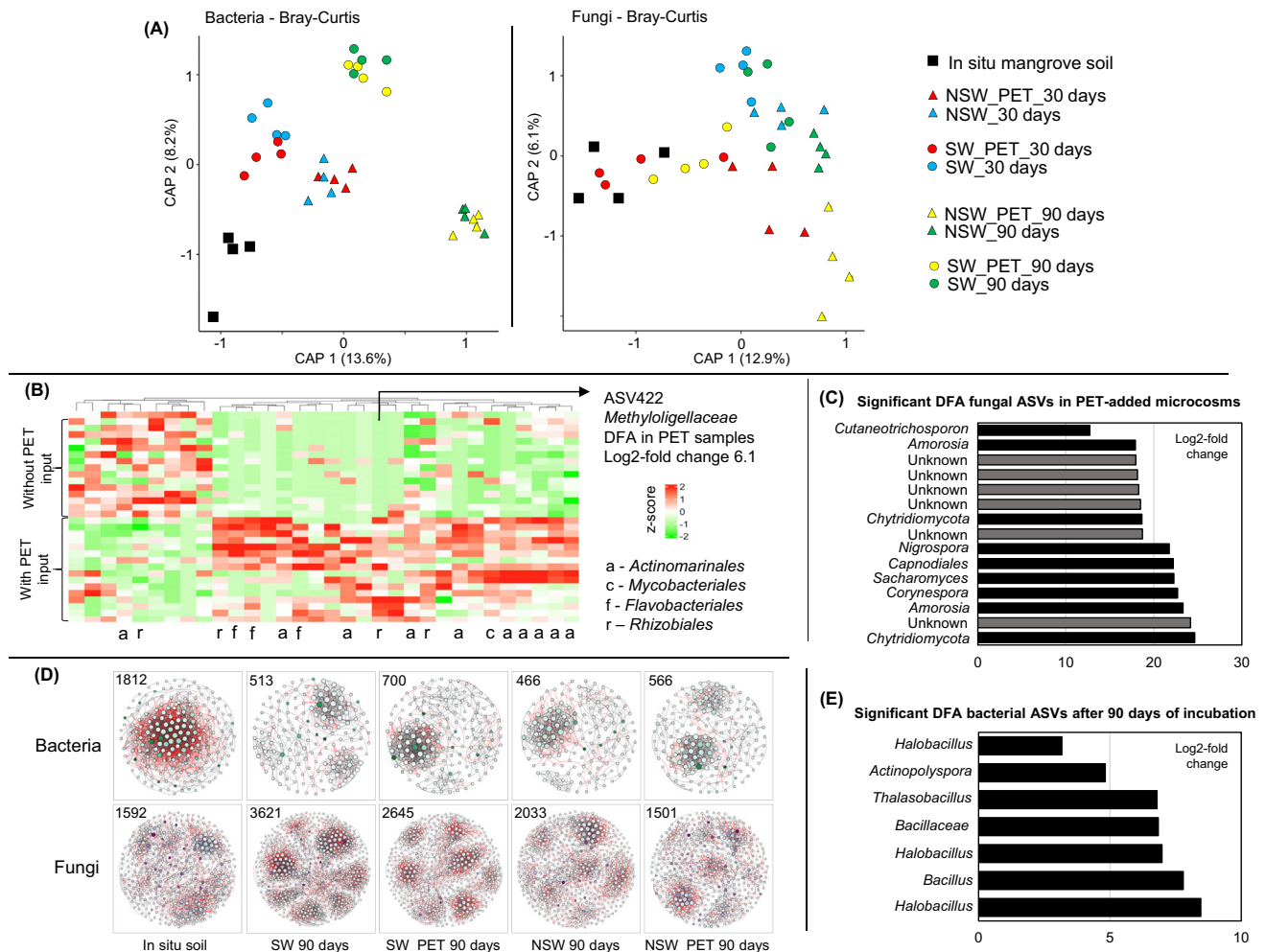
A microcosm experiment was performed to evaluate the effects of amorphous PET copolyester particles (<5 mm in size) on the mangrove soil microbiome along with two environmental factors. First, the inclusion of seawater was used to mimic the sea-level rise, a factor that directly affects the input of external nutrients and the dispersal of microbial taxa. Second, the time of incubation (i.e., 30 and 90 days) at 30°C was used to generate a gradient of soil desiccation that may be expected with shifting flooding events and precipitation regimes under projected climate change scenarios (Figure 1A).

Our results showed that seawater input had a major impact on the mangrove soil microbiome structure, resulting in a distinct microbial community after 90 days of incubation (Figure 2A). This occurred due to the shift in abiotic conditions combined with the input of taxa via dispersal



Trends in Biotechnology

Figure 1. Schematic of the experimental approaches in this study. (A) A mangrove soil microcosm experiment was set up to assess the effects of polyethylene terephthalate (PET) particles and seawater (SW) intrusion on the soil microbiome after 30 and 90 days of incubation at 30°C. Soil desiccation was evident after 90 days. (B) A top-down selection strategy was used to develop PET-transforming bacterial consortia from a perturbed mangrove soil microbiome. T1–T6 refer to the transfer number in the dilution-to-stimulation approach. T3R3 refers to replicate 3 in transfer 3. Microbial transformation of PET was evaluated after T6 using Fourier-transform infrared spectroscopy (FTIR), thermogravimetric analysis (TGA), and differential scanning calorimetry (DSC). Abbreviations: MSM, mineral salt medium; TE, trace elements solution; VS, vitamin solution.



Trends in Biotechnology

Figure 2. Bacterial and fungal community analysis in the soil microcosm experiment. (A) Canonical analysis of principal coordinates (CAP) of Bray–Curtis distances of bacterial and fungal communities. Circles indicate samples with seawater input; triangles indicate samples without seawater input; red and yellow circles and triangles indicate microcosm samples with the inclusion of polyethylene terephthalate (PET) microparticles; blue and green circles and triangles indicate samples with no PET particles. (B) Heat-map of normalized relative abundance (z-score) of selected amplicon sequence variants (ASVs; columns) that explained variations between PET and non-PET-added soil microcosms (rows). ASVs belonged to other taxa are unlabeled. A significantly differentially abundant taxon, namely ASV422, is indicated by an arrow. (C) Log-fold change values of the significantly differentially abundant fungal ASVs in the PET-added microcosms. Fungal ASVs without confident taxonomic assignment are indicated in gray. (D) Co-occurring bacterial and fungal networks comparing all soil microcosms after 90 days of incubation against the *in situ* mangrove soil communities. The numbers inside the boxes correspond to the number of edges (a proxy value of complexity). (E) Comparison of log₂-fold change values of the significantly differentially abundant bacterial ASVs in the microcosms between 90 and 30 days of incubation. Abbreviations: DFA, differentially abundant; NSW, non-seawater; SW, seawater.

(i.e., ‘community coalescence’), a phenomenon that remains overlooked in mangrove soils ecosystems but may have a pivotal role in buffering microbial diversity and restoring key functions after an environmental perturbation [43–46]. Although the input of PET particles did not lead to large shifts in bacterial community structure, there were significant differences ($P = 0.003$, $R^2 = 0.042$) between the control and PET treatments. These differences were more pronounced for fungal communities ($P = 0.0003$, $R^2 = 0.063$). Owing to the short timeframe of our experiment and recalcitrance of PET, the changes observed were likely associated with the physical modification of soil structure rather than to the presence of PET as an external carbon source [47].

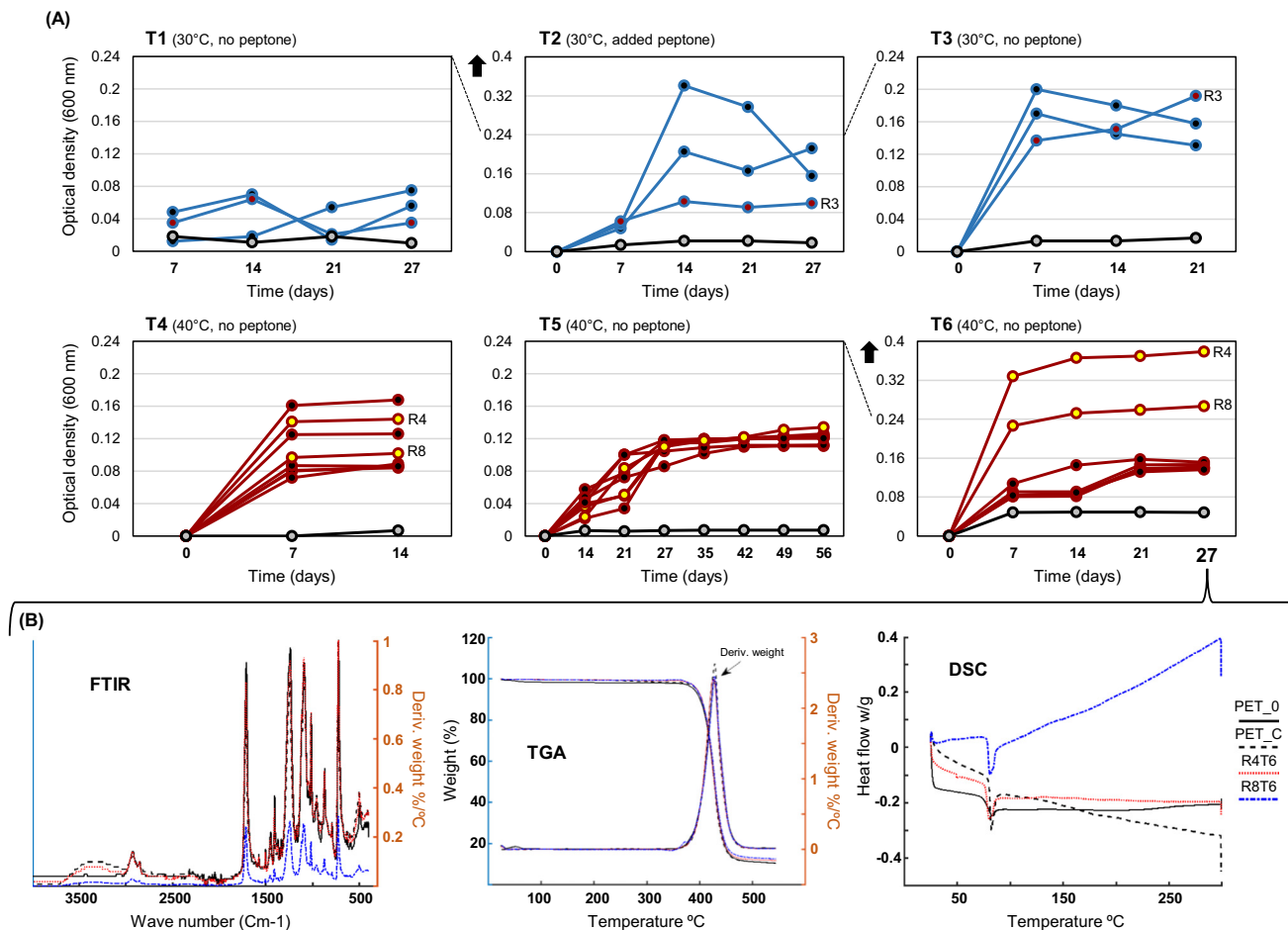
Differential abundance analysis revealed 32 bacterial amplicon sequence variants (ASVs), which explained the differences between the negative controls and PET treatments. Most ASVs were affiliated to the orders *Actinomarinales*, *Mycobacteriales*, *Flavobacteriales*, and *Rhizobiales*. Of these, only one ASV (belonging to the *Methyloligellaceae*) was significantly enriched in the PET-added microcosms (DESeq2; $P < 0.0001$) (Figure 2B). Notably, members of this family are colonizers of various types of plastic in marine environments [48–50]. We also observed a significant enrichment of fungal ASVs in PET-added microcosms, most of which were assigned to unknown taxa (Figure 2C). Furthermore, a co-occurrence network analysis suggested that, compared with *in situ* soil communities, the complexity of bacterial communities (defined herein as the number of edges and nodes) was reduced in the microcosms after 90 days of incubation; this decrease in complexity was most evident in treatments without seawater. By contrast, the complexity of fungal communities increased in the microcosms containing seawater after 90 days of incubation (Figure 2D and Table S1 in the supplemental information online). Interestingly, seven ASVs, mostly belonging to halophilic bacterial genera (e.g., *Halobacillus* and *Thalassobacillus*), were significantly enriched (DESeq2; $P < 0.00001$) across all treatments after 90 days of incubation compared with those after 30 days of incubation (Figure 2E). This suggested that drought conditions intensified over time in our soil microcosms, resulting in a greater effect of salinity as a variable imposing selection on specific salt-adapted bacterial taxa. That is, soil desiccation increased salinization in the microcosms, which imposed an environmental filtering effect on bacterial and fungal taxa and their interactions [20], thereby potentially changing the landscape of the co-occurrence network. However, it is plausible that seawater intrusion exerts an effect on fungal interactions, which may be caused by the dispersal of taxa into the system [51].

Artificial selection of microbial consortia involved in PET transformation

To artificially select microbial communities capable of PET degradation, the microbiota from the microcosm incubated for 90 days with PET particles and seawater was used as the inoculum source for subsequent enrichment liquid cultures containing PET as the sole carbon source. This microbial inoculum was selected based on its longer exposure time to PET particles and higher bacterial complexity compared with other treatments (Figure 2D). This reshaped mangrove soil microbiota was subjected to individual-level selection using sequential growth cycles [34,38,40] over six transfers (T1–T6), with specific shifts in culture conditions (Figures 1B and 3A; see STAR★METHODS).

During T1, no significant cell growth [based on optical density at 600 nm (OD_{600})] was observed compared with the negative controls (Figure 3A). Therefore, we added peptone (a protein hydrolysate) to T2 to favor microbial growth in the presence of PET particles. The addition of protein hydrolysate to culture media was originally reported for the selection of poly(butylene adipate-co-terephthalate)-degrading microbial consortia [52]. Compared with the microbial inoculum from the soil microcosm (i.e., SW_PET 90 days), bacterial alpha diversity was reduced after T2 (Figure 4A). The inclusion of peptone increased the cell density and relative abundance of *Pseudomonas* and *Sphingobium* spp. within the selected community after 27 days of incubation at 30°C (Figures 3A and 4B). Peptone was not added during T3, and the microbial populations showed reduced growth compared with that during T2 but higher growth compared with that during T1. After T3, peptone was depleted due to its consumption and subsequent dilutions along the transfers.

Subsequently, the biological replicate with the highest growth (i.e., replicate 3, R3) was used as a microbial seed for subsequent growth cycles at 40°C. This increase of 10°C aimed to enhance microbial activity and PET flexibility, thereby favoring plastic degradation and growth [53]. Eight biological replicates were set up at T4, and similar absorbance values were observed compared with those at T3 after 14 days of incubation (Figure 3A). Then, the community structure trajectories of

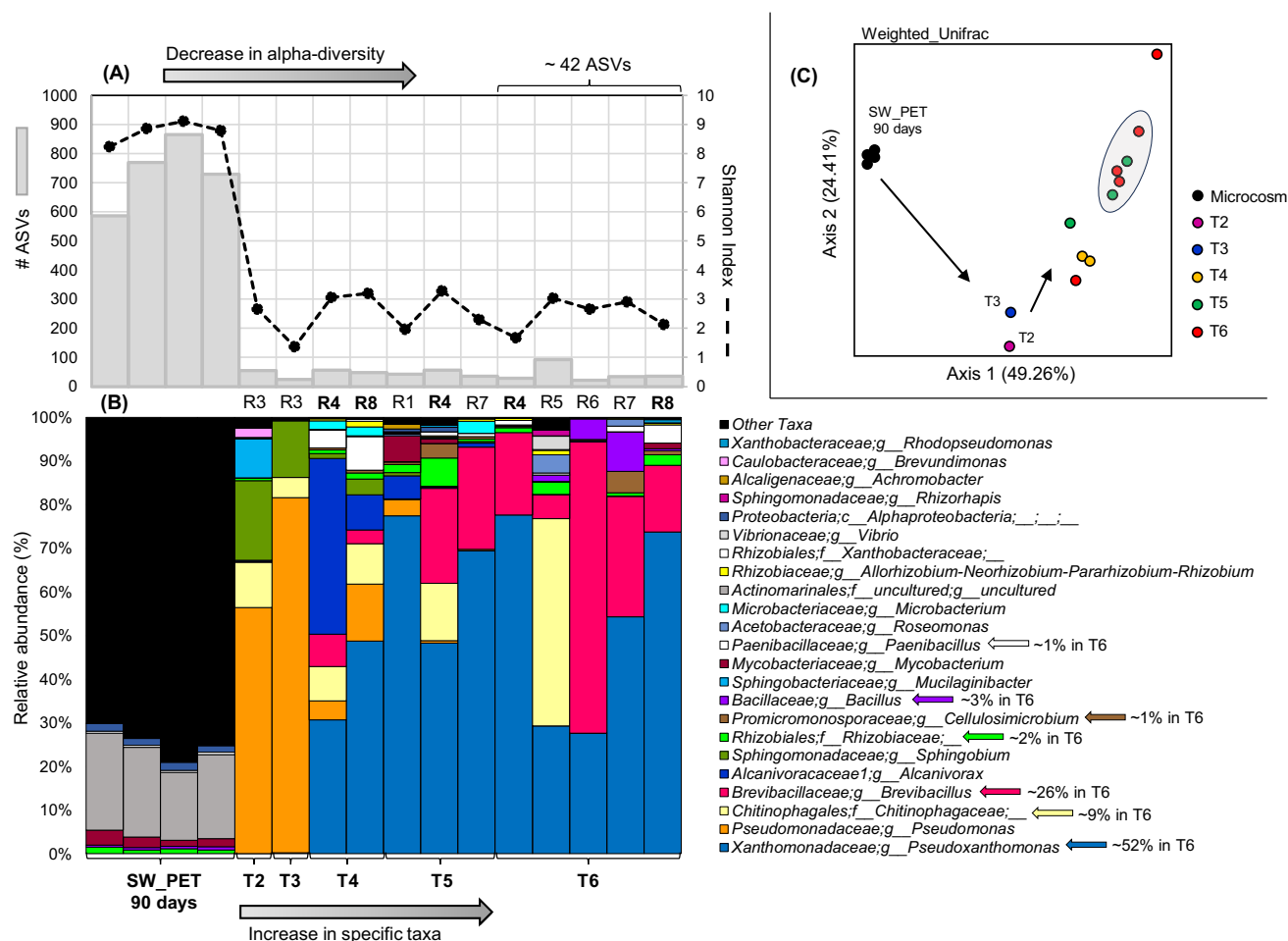


Trends in Biotechnology

Figure 3. Analyses during the artificial selection of polyethylene terephthalate (PET)-transforming bacterial consortia. (A) Values of the growth [optical density at 600 nm (OD_{600})] of microbial communities within each transfer during the top-down selection strategy. From T1 to T3, three biological replicates (in blue) were present compared with the negative control (flask without microbial source indicated by a black line). Replicate R3 is shaded with red dots. From T4 to T6, eight biological replicates (in red) derived from replicate 3 (R3) after T3. Microbial consortia R4T6 and R8T6 are shaded with yellow dots. Black arrows on the y-axis indicate the scale increase up to 0.4. (B) Profiles of Fourier-transform infrared spectroscopy (FTIR), thermogravimetric analysis (TGA), and differential scanning calorimetry (DSC). Red and blue broken lines represent data from PET particles obtained in T6 after 27 days of incubation with R4T6 and R8T6 bacterial consortia, respectively. PET_0 and PET_C refer to negative controls.

replicate R4 (the best-performing consortium based on OD_{600}) were compared with those of other replicates communities. The bacterial community structure drastically changed after T4 (Figure 4C), with increases in the relative abundance of *Alcanivorax*, *Paenibacillus*, and *Pseudoxanthomonas* spp. (Figure 4B). *Alcanivorax* spp. are some of the most studied oil-degrading microorganisms and can potentially biodegrade PE, polypropylene (PP), and PET [36,54,55].

During T5, the incubation period was prolonged to 56 days to enhance microbial growth rates, thereby favoring slow-growing bacterial species. However, there was no significant increase in the absorbance values after 35 days of incubation (Figure 3A). This prolonged incubation period favored an increased relative abundance of *Brevibacillus* sp., *Cellulosimicrobium* sp., and members of the *Rhizobiaceae*, especially in R4 (Figure 4B). A relatively longer incubation time often favors the growth of oligotrophic and slow-growing bacterial taxa [56,57] that are potential PET degraders. However, excessively long incubation times may enhance the growth of microbial



Trends in Biotechnology

Figure 4. Bacterial diversity analysis from the resulting polyethylene terephthalate (PET)-transforming consortia. (A) Bacterial alpha diversity [number of amplicon sequence variants (ASVs) and Shannon index] during the successive transfers of the top-down selection strategy. Each bar represents biological replicates of the initial inoculum in the microcosm (SW_PET 90 days) and the sequential transfer (T1–T6). (B) Genus-level relative abundance of the taxa in the sequential transfers during the artificial selection strategy. Colored arrows (right) indicate the most abundant taxa after T6. (C) Principal coordinate analysis (PCoA) plot based on weighted UniFrac distances showing the bacterial community similarity between soil inoculum (SW_PET 90 days) and the selected bacterial consortia along the transfers (T1–T6).

species that are not directly associated with PET transformations, such as those related to the consumption of byproducts (e.g., dead cells) generated in the system [34]. Beta-diversity analysis (Figure 4C) revealed that the enriched bacterial communities from T5 and T6 were similar, suggesting that the consortia had reached an equilibrium state. However, subsequent transfers can likely reshape the community structure due to stochastic process (e.g., priority effects and ecological drift of low abundant taxa).

During T6, the absorbance values were >0.24 for R4 and R8 after 14 days (Figure 3A), indicating increased growth over the incubation period. After T6, 28 and 35 bacterial ASVs were obtained from R4 and R8, respectively. Based on the relative abundance of 16S rRNA genes, these two bacterial consortia (referred to hereafter as R4T6 and R8T6) comprised primarily *Pseudoxanthomonas* sp. (average, 60%) and *Brevibacillus* sp. (average, 20%) (Figure 4A,B). Although *Pseudoxanthomonas* has not yet been described as a PET-depolymerizing microorganism, recent evidence indicated its ability to grow in consortia on chemically deconstructed

PET [58,59]. Furthermore, according to a previous study, a consortium mostly comprising *Brevibacillus* spp. transformed PE and PP [60].

Evidence of PET biotransformation

After the growth of the R4T6 and R8T6 consortia, the remaining PET particles were collected to evaluate structural changes in the polymer via Fourier-transform infrared spectroscopy (FTIR), thermogravimetric analysis (TGA), and differential scanning calorimetry (DSC) (see STAR★METHODS). FTIR has been used previously to evaluate PET degradation mechanisms in marine systems [61]. When using FTIR, an increase in the carbonyl-index is interpreted as a signal associated with PET biodegradation [62]. In addition, changes in temperature associated with weight losses (as detected by TGA) also indicate plastics transformation [63], whereas variation in the glass transition temperature (detected by DSC) can indicate deconstruction in polymeric chains [62].

In our study, the FTIR spectrum showed distinctive peaks of PET, and the ratio of the absorbance peak in the 1715 cm^{-1} band to the peak at 1505 cm^{-1} (i.e., carbonyl-index) was increased in R8T6 (8.0) compared with that in the control containing PET in a cell-free culture medium (PET_C; 6.1) and the control containing untreated PET (PET_0; 6.5) (Figure 3B), suggesting structural modification of the polymer. As expected, TGA showed that all PET samples exhibited a large weight loss at $\sim 430^\circ\text{C}$, corresponding to the thermal decomposition of PET [64]. Compared with the negative controls, this temperature was slightly reduced for PET from R4T6 (426.7°C). DSC analysis showed a reduction in glass transition temperatures in R4T6 (79.7°C) and R8T6 (81.6°C) compared with those in PET_0 (83°C) and PET_C (82.1°C).

Collectively, our results indicated the increased mobility of PET chain segments and slight transformation of PET due to microbial activity of the consortia (Figure 3B). However, this evidence is indirect and not enough to support the complete PET biodegradation (i.e., polymer deconstruction and assimilation of monomers). Recently, several methods have been used to explore PET biotransformation (e.g., microscopy, microbial growth, thermal analysis, weight losses, and detection of monomers). Each of these approaches have pros and cons that must be considered carefully [65]. Unfortunately, there is still not a golden standard protocol to investigate plastics transformation [11]. However, to obtain direct evidence of complete PET biodegradation the use of isotopic labeling (e.g., stable isotope ^{13}C -labeled PET) is recommended [65,66].

Analysis of metagenome-assembled genomes from the PET-transforming bacterial consortia

Metagenome sequencing of R4T6 and R8T6 microbial consortia yielded a total of 11.71 and 12.76 Gbp, respectively. Taxonomic classification using the metagenome classifier Kaiju revealed that $\sim 85\%$ of the sequences were associated with *Xanthomonadales*, while the remaining reads were affiliated with *Bacillales*, *Rhizobiales*, *Mycobacteriales*, and other bacterial orders. These two bacterial consortia were also subjected to a genome-centric metagenomic analysis, resulting in the recovery of three and seven high-quality metagenome-assembled genomes (MAGs) (i.e., completeness $\geq 90\%$ and contamination $\leq 5\%$) from R4T6 and R8T6, respectively. Approximately 97% of R4T6 and R8T6 raw sequences were mapped to these ten MAGs, indicating the reconstruction of an important fraction of the entire bacterial consortia. The DNA G+C content, number of protein coding genes, and other genomic features are summarized in Table 1.

Taxonomic assignment based on average nucleotide identity (ANI) values revealed that most MAGs belonged to known species (Table 1), with three MAGs representing novel species of the genera *Kaistia* and *Mesorhizobium* [*Mesorhizobium*_H in Genome Taxonomy Database (GTDB)]. Based on read counts per kilobase (of genome) per million (bases of recruited sequences) (RPKM median values), the most abundant member in R4T6 was *Pseudoxanthomonas*

Table 1. Features of high-quality MAGs derived from R4T6 and R8T6 bacterial consortia^a

MAG ID	RPKM	Completeness	Contamination	No. of contigs	Genome size (Mbp)	No. of proteins	GC	Taxonomy classification ^b	CP genome	CP ANI
R4T6										
MAG_4_P4	206.7	95	1.7	93	4.993252	4951	0.52	<i>Brevibacillus borstelensis</i>	GCF_003710865.1	99.51
MAG_5_P4	222.6	99.66	0.43	39	4.435419	3764	0.69	<i>Pseudoxanthomonas winnipegensis</i>	GCF_004284195.1	97.56
MAG_9_P4	191.1	99.55	0.55	30	4.586290	4393	0.63	<i>Mesorhizobium</i> sp.	GCF_009749525.1	83.37
R8T6										
MAG_001_P8	222.6	99.66	0.43	66	4.428494	3763	0.69	<i>P. winnipegensis</i>	GCF_004284195.1	97.54
MAG_11_P8	115.8	96.64	0.95	278	4.551535	4444	0.68	<i>Kaistia</i> sp.	GCA_017307955.1	93.51
MAG_0_P8	185.4	99.73	1.84	63	5.544610	5302	0.54	<i>Brevibacillus agri</i>	GCF_004117055.1	99.2
MAG_004_P8	144	99.81	0.63	98	6.269040	6084	0.66	<i>Mycolicibacterium fortuitum</i>	GCF_000295855.1	98.64
MAG_005_P8	142.9	99.83	1.79	166	5.803327	5304	0.65	<i>Rhodopseudomonas pseudopalustris</i>	GCF_003591005.1	97.37
MAG_14_P8	172.3	100	0.67	384	4.334234	4055	0.75	<i>Cellulosimicrobium funkei</i>	GCF_004519295.1	97.26
MAG_11A_P8	203.5	99.55	0.55	29	4.603441	4404	0.63	<i>Mesorhizobium</i> sp.	GCF_009749525.1	83.39

^aAbbreviations: ANI, average nucleotide identity; CP, closest placement; RPKM, read counts per kilobase (of genome) per million (bases of recruited sequences).

^bTaxonomic classification performed via ANI using the GTDB database.

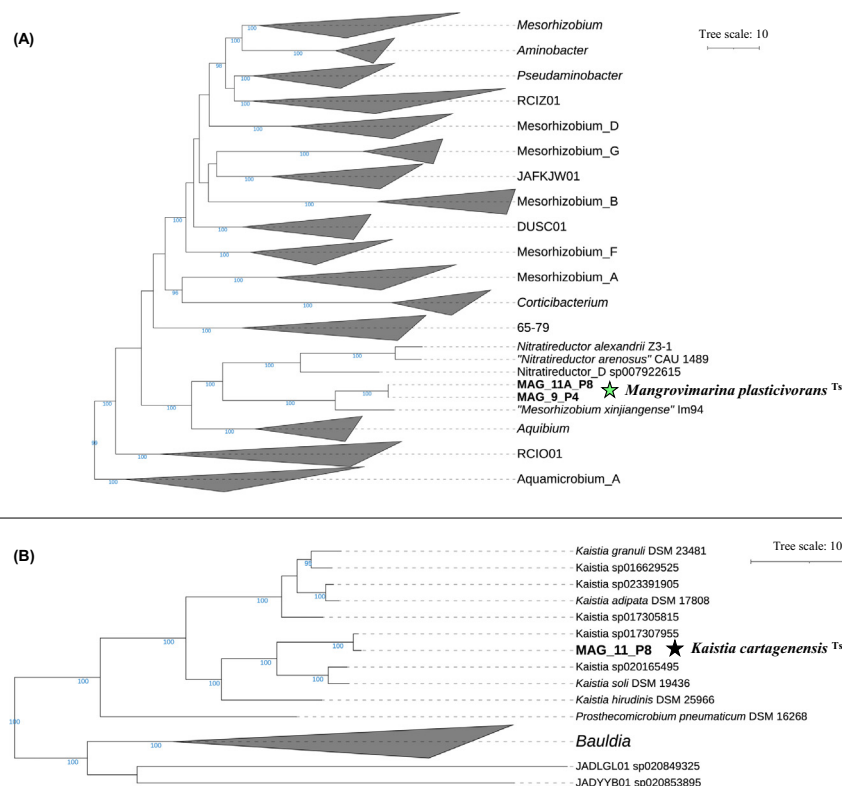
winnipegensis, whereas in R8T6, *P. winnipegensis*, *Brevibacillus agri*, and *Mesorhizobium* sp. were the most dominant (Table 1). Interestingly, MAGs belonging to *P. winnipegensis* (MAG5_P4 and MAG001_P8) and *Mesorhizobium* sp. (MAG9_P4 and MAG11A_P8) were found in both biological replicates, suggesting these organisms as key players in PET catabolism. In fact, ASVs classified as *Mesorhizobium* were reported as enriched in a terephthalate-consuming consortium [58]. Additionally, MAGs belonging to *Cellulosimicrobium funkei*, *Kaistia* sp., *Mycolicibacterium fortuitum*, and *Rhodopseudomonas pseudopalustris* were detected in R8T6 (Table 1). *Rhodopseudomonas* sp. has been reported to have the enzymatic potential to break down polyesters and to colonize and degrade PE films [67,68].

As mentioned earlier, MAGs affiliated with *Kaistia* sp. and *Mesorhizobium* sp. showed ANI values <95% against the closest representative genomes in GTDB (Table 1), thus representing novel bacterial species. The average amino acid identity (AAI) scores revealed a distant relationship of MAG9_P4 and MAG11A_P8 with *Mesorhizobium oceanicum* (GCF_001889605.1, 64.38%) and *Nitratireductor arenosus* (GCF_009742725.1, 63.26%), suggesting that these taxa belonged to a novel genus within the order Rhizobiales [$P = 0.0018$, highest taxonomic rank with $P \leq 0.01$ based on the Microbial Genomes Atlas (MiGA)]. This was supported by the GTDB classification, which placed MAG9_P4 and MAG11A_P8 along with '*Mesorhizobium xinjiangense*' into a distinct genus, *Mesorhizobium_H* (Table 1). In addition, a low digital DNA–DNA hybridization (dDDH) value (25.5%) was obtained against '*M. xinjiangense*' Im94T. According to the phylogenomic trees based on Genome BLAST Distance Phylogeny (GBDP) distances (Figure S1 in the supplemental information online) and 120 concatenated single-copy protein genes (Figure 5A), MAG9_P4 and MAG11A_P8 were closely related to *Nitratireductor mangrovi* SY7 (*Nitratireductor_D* sp007922615 in GTDB) and formed a well-supported cluster with '*M. xinjiangense*' Im94T (Figure 5A). '*M. xinjiangense*' Im94T was isolated from the rhizosphere soil of *Alhagi sparsifolia* [69], a shrub species that thrives in saline and desert soils in China [70]. Moreover, *Nitratireductor* species have been frequently found in mangroves or polluted saline soils [71–73]. These previous reports support the hypothesis that the proposed novel genus is adapted to saline soils, such as those in our microcosm experiment. Furthermore, phylogenomic trees supported the affiliation of another novel species found in this study, represented by MAG11_P8, with the *Kaistia* genus (Figure 5B and Figure S1). Thus, based on the genomic characteristics and phylogenetic analyses, MAG11_P8 and MAG pair MAG9_P4/MAG11A_P8 are likely to represent novel species, for which the following names are proposed: *Kaistia cartagenensis* sp. nov. (type material genome sequence GCA_963966455 deposited in GenBank) and *Mangrovimarina plasticivorans* gen. nov., sp. nov. (type material is a genome sequence GCA_963966365 deposited in GenBank), respectively.

All species and genus names proposed in this study have been submitted to the SeqCode registry [74] under register list <https://seqco.de/r:ayug-nu6>; and their etymology is as follows: (i) *K. cartagenensis* (car.ta.ge.nen'sis. N.L. fem. adj. *cartagenensis*, pertaining to Cartagena de Indias, the city close to Barú peninsula, where the mangrove soil samples were taken to build up the microcosms experiment); (ii) *Mangrovimarina* (Man.gro.vi.ma.ri'na. N.L. neut. n. *mangovum*, a mangrove; L. fem. adj. *marina*, marine; N.L. fem. n. *Mangrovimarina*, referring to an organism found in mangrove soils with seawater impact); and (iii) *M. plasticivorans* (plas.ti.ci.vo'rans. N.L. neut. n. *plasticum*, plastic; L. pres. part. *vorans*, devouring, destroying; N.L. part. adj. *plasticivorans*, plastic devouring, referring to ability of an organism to catabolize plastic).

Interactive bacterial catabolism of PET-derived monomers

To elucidate the functional role of each species within the R4T6 and R8T6 bacterial consortia, we searched for genes involved in PET catabolism for each MAG (Figure 6A and Table S2 in the supplemental information online). None of the MAGs harbored close gene homologs to K21104



Trends In Biotechnology

Figure 5. Phylogenetic position of novel metagenome-assembled genomes (MAGs). (A) MAG9_P4 and MAG_11A_P4. (B) MAG_11_P8. The maximum-likelihood trees were inferred using the concatenated alignment of 120 single-copy proteins among the closely related members of the *Rhizobiaceae* (A) and *Kaistiaceae* (B), using IQ-TREE and genomic sequences from Genome Taxonomy Database (GTDB) RS-R214. Trees were rooted with outgroups (not shown) and visualized using iTOL.

(PETase from *I. sakaiensis*) and K18075 (terephthalate 1,2-dioxygenase oxygenase; gene *tphA3*). However, MAG9_P4 and MAG11A_P8 (from novel species *M. plasticivorans*) contained two proteins homologous to K21105 (MHETase from *I. sakaiensis*) (Figure 5A). These two putative MHETases were compared via BLAST with the National Center for Biotechnology Information (NCBI) database, and the best matches corresponded to a tannase/feruloyl esterase family alpha/beta hydrolase (64% and 82% identity against WP_157015687, respectively). Based on Kyoto Encyclopedia of Genes and Genomes (KEGG) Orthology (KO) assignments, *M. plasticivorans* and *R. pseudopalustris* have the genomic potential to catabolize TPA into protocatechuic acid (Figure 6A,B and Table S2) because they harbor *tphA* (K18074 and K18077) and *tphB* (K18076) [75]. *Rhodopseudomonas* sp. and *Mesorhizobium* sp. have been reported to be significantly enriched in consortia that grow on PET-derived substrates [76]. Interestingly, only *M. fortuitum* contained homologous proteins (propanediol dehydratases; K13919 and K13920) involved in the conversion of EG into acetaldehyde (Figure 6A, and Table S2), suggesting its importance as a specialist in the R8T6 consortium. In addition, *P. winnipegensis*, *M. plasticivorans*, *R. pseudopalustris*, and *K. cartagenensis* contained homologous proteins involved in the conversion of EG into glycolaldehyde. Furthermore, in the MAGs associated with *Brevibacillus* spp. (i.e., MAG4_P4 and MAG0_P8), we found homologous proteins involved in the conversion of TPA-*cis*-1,2-dihydrodiol and glycolaldehyde (Figure 6A,B and Table S2). Collectively, these findings suggest that the catabolism of PET-derived monomers in R4T6 and R8T6 occurs via interactive metabolic processes across distinct taxa. Similar

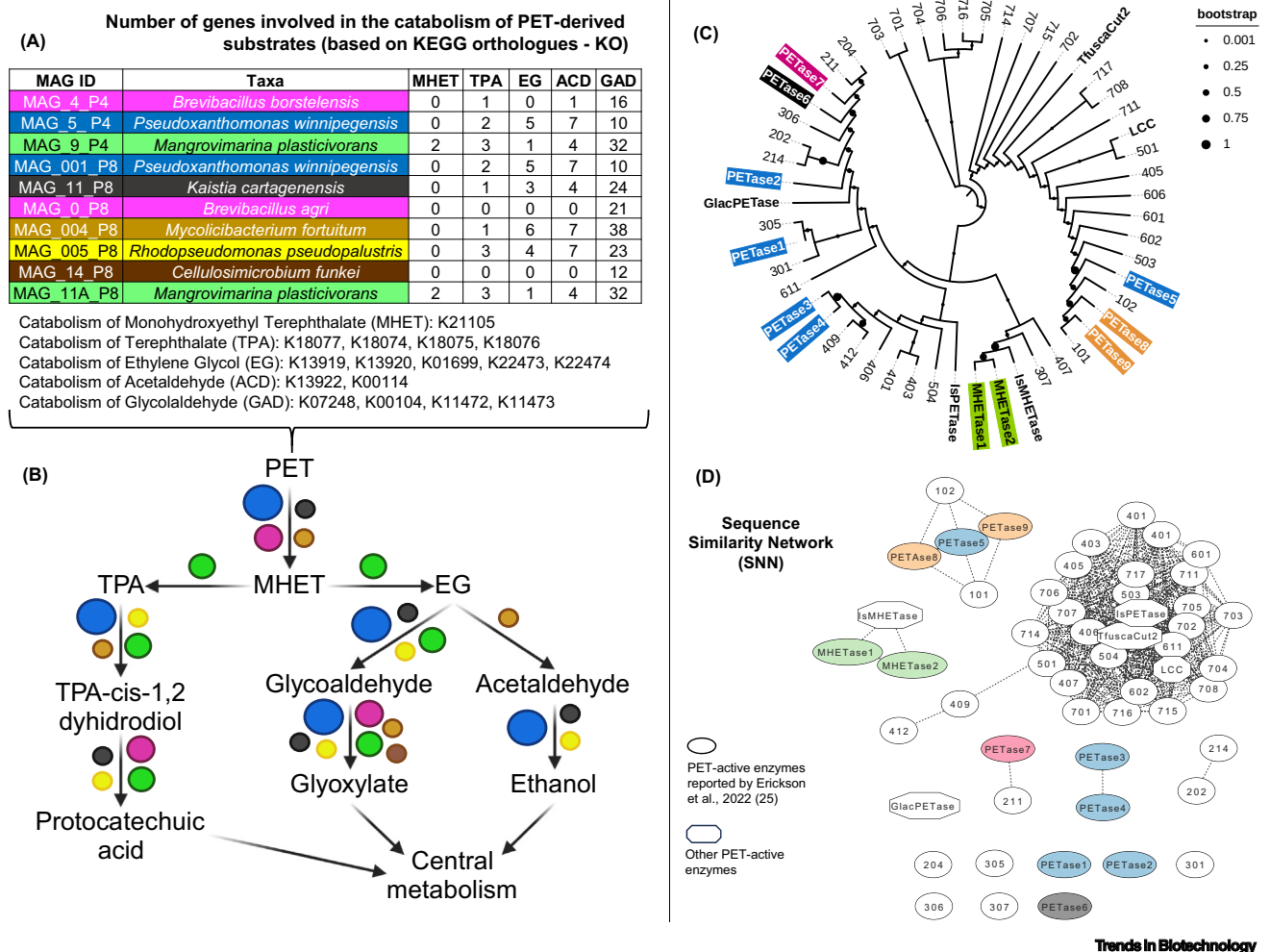


Figure 6. Analysis of polyethylene terephthalate (PET)-transforming enzymes obtained from the bacterial consortia. (A) Number of genes involved in PET catabolism within metagenome-assembled genomes (MAGs) retrieved from R4T6 and R8T6 bacterial consortia. Genes were detected via KofamKOALA functional annotation using Kyoto Encyclopedia of Genes and Genomes (KEGG) Orthology (KO) identifiers and a cutoff of 100 in the Hidden Markov Model scores. (B) Schematic of PET catabolism within the R4T6 and R8T6 consortia and the species involved in each step. This figure was constructed using the KEGG functional annotation [displayed in (A)] and the annotation obtained using the Plastic-Active Enzymes (PAZy) database. Each color represents a genus that matches with the colors in (A) (i.e., blue, *Pseudoxanthomonas*; green, *Mesorhizobium*; pink, *Brevibacillus*; orange, *Mycolicibacterium*; yellow, *Rhodopseudomonas*; black, *Kaistia*; brown, *Cellulosimicrobium*). Circle sizes represent the relative abundance of each MAG within the R4T6 and R8T6 consortia. (C) Phylogenetic tree of the predicted PET hydrolases (PETases) found in the MAGs from the R4T6 and R8T6 consortia. Colors represent the bacterial origin of the enzyme (as mentioned earlier). The bootstrap consensus tree was inferred from 1000 replicates. Branches corresponding to partitions reproduced in <50% bootstrap replicates were collapsed. (D) Sequence similarity network (SSN) of experimentally confirmed PET-active hydrolases found by Erickson and colleagues [25], including IsMHETase [23], GlacPETase [26], and putative active PETases and monohydroxyethyl terephthalate (MHET) hydrolase (MHETase) identified in this study. Edges represent pairwise BLAST similarity with an *E*-value of <1e-10. The SSN clusters are consistent with the phylogenetic groups in (C).

evidence was recently reported from sediment-derived microbial consortia, where the catabolism of PET-derived substrates depended on the coexistence of specialists and generalists [58,59]. However, these conclusions are based on the genomic potential of bacterial species, and further experiments (e.g., metatranscriptomic or metaproteomic analysis) would be useful to confirm these results.

Detection of putative novel PET-degrading enzymes

Putative PETases were searched within the MAGs using the Plastic-Active Enzymes (PAZy) database [77]. MAGs from *P. winnipegensis* (MAG5_P4 and MAG001_P8) contained five putative

PETases with Hidden Markov Model (HMM) scores of 71.9–82.3. These enzymes were compared against the NCBI database, and the best matches corresponded to alpha/beta-fold hydrolases, carboxylesterases, and S9 family peptidases (Table S3 in the supplemental information online). Additionally, four putative PETases, with HMM scores between 74.7 and 76.4, were detected in MAGs from *K. cartagenensis*, *B. agri*, and *M. fortuitum*. These nine putative PETases (Table S4 in the supplemental information online) did not show the large motif M5 that is present in the PETase of *I. sakaiensis* [78]. Signal peptides were found in PETases 1–8, suggesting that they are secreted by the bacteria. Although the HMM scores were low compared with the reported PET-active enzymes, it has been demonstrated that alpha/beta-fold hydrolases (e.g., carboxylesterases and peptidases) with HMM scores <55 had catalytic activity on PET [25]. The nine putative PETases and the two MHETases detected in the MAGs from R4T6 and R8T6 (Table S4) were compared with 42 enzymes with confirmed catalytic activity on PET using phylogenetic analysis (Figure 6C). PETase 5 (derived from *P. winnipegensis*) and PETases 8 and 9 (derived from *M. fortuitum*) clustered together with PETases 101 and 102, which belong to a new family of PET-active enzymes derived from thermophilic environments [25]. This result was consistent with our sequence similarity network (SSN) analysis (Figure 6D). Specifically, PETase 5 showed 53% identity (88% coverage) with PETase 102, and PETase 8 showed 44% identity with PETase 101 (78% coverage). As expected, MHETases 1 and 2 (from *M. plasticivorans*) clustered together with MHETase from *I. sakaiensis* (IsMHETase). Both proteins showed ~40% identity (83% coverage) with IsMHETase. Based on the SSN analysis (Figure 6D), PETase 7 (from *B. agri*) shared a similarity of >35% to protein 211, another active PETase detected by Erickson and colleagues [25]. Although PETases 1, 2, 3, and 4 (from *P. winnipegensis*) did not cluster with any PET-active enzymes (Figure 6D), PETase 1 showed a similarity of 28% (with 41% coverage) to a GlacPETase derived from *Pseudomonas* sp. from a glacier microbiome [26]. These results provide initial evidence for the discovery of novel bacterial PET-transforming enzymes from mangrove soil microbiomes. Further studies and experiments, such as chemical synthesis, gene cloning and expression, protein purification and determination of enzymatic activities, will be needed to validate these findings [79].

Concluding remarks

The results obtained from the soil microcosm experiment supported four main conclusions. First, the input of seawater significantly affected the mangrove soil microbiome due to shifts in abiotic and biotic properties in our system; this was associated with the input of nutrients and organisms via dispersal. Second, the desiccation of mangrove soils affected nonhalotolerant bacterial species. Third, the inclusion of PET particles only caused small changes in the soil microbiome structure, although this may have been due to the short timeframe of our experiment. Fourth, at the end of the microcosm experiment, novel restructured microbial communities were obtained. These findings provide new insights toward a better understanding of the mangrove soil microbiota under the direct influence of plastics particles along other environmental conditions.

Moreover, our strategy of combining mangrove soil microcosms with enrichment cultures was successful in selecting PET-transforming bacterial communities. Our top-down strategy and the modification of culture conditions along six growth cycles enhanced the growth of mangrove-derived bacterial taxa in a culture medium containing PET as the sole carbon source. This led to the artificial selection of novel PET-transforming consortia, mostly comprising *Pseudoxanthomonas winnipegensis*, *Brevibacillus* spp., and a novel bacterial taxon (*Mangrovimarina plasticivorans* gen. nov. sp. nov.). These PET-transforming species will be targeted for upcoming isolation tests. We foresee that information obtained from MAGs on nutritional needs and functional traits could assist the design of strategies to obtain pure cultures of functional taxa from the consortia. Moreover, MAG analyses supported PET catabolism as an interactive effort,

Outstanding questions

Does the process of PET depolymerization and mineralization require the activities of different microbial groups (e.g., fungi or bacteria) in natural ecosystems?

What are the potential co-metabolisms between microbial taxa associated with PET transformation in natural ecosystems?

Can the stable isotope probe technique be a suitable approach to identify microbial taxa involved on catabolism of PET and its monomers?

What other engineering strategies can be combined with our selective enrichment for optimizing microbial consortia for PET transformation?

Can long-term evolutionary assays enhance the efficiency of a preselected microbial consortium for PET transformation?

What proteins are expressed and secreted during the selection of PET-transforming microbial consortia in enrichment cultures?

Does the level of microbial diversity in a consortium affect the efficiency of PET degradation?

How can we use engineering microbiomes to enhance PET bioremediation in natural ecosystems?

How can we isolate novel PET-degrading microorganisms using information retrieved from their genomes?

wherein some species may deconstruct PET and others could participate in the catabolism of PET-derived substrates.

Even though microplastics bioremediation in nature remains challenging (due to low effectiveness, problems with scalability, implementation, evaluation, etc.; see [Outstanding questions](#)), our study provides new information for the design of microbial inoculants and/or enzyme cocktails able to enhance or accelerate PET degradation in marine ecosystems. Our selective strategy can be expanded to other ecosystems (e.g., freshwater, saltmarsh soils, or forest soils), which could result in the discovery of new plastic-degrading microbes. The broad use of this approach will help research developments toward designing efficient minimal microbial communities targeting plastics transformation in both the laboratory and large-scale industrial settings. In summary, our study provides a valuable approach for harnessing soil microbiomes, leading to the development of strategies for the selection of PET-degrading microbial communities with the potential to discover new enzymes useful for PET transformation.

STAR★METHODS

Detailed methods are provided in the online version of this paper and include the following:

- KEY RESOURCES TABLE
- METHOD DETAILS
 - Setup of soil microcosm experiments
 - Microbial diversity analyses from the microcosms
 - Artificial selection strategy
 - Bacterial diversity during enrichment cultures
 - Assessments of PET structural changes
 - Assembly of metagenomes
 - Taxonomic and phylogenetic analysis of MAGs
 - Detection of putative plastic-active enzymes
 - Analysis of putative plastic-active enzymes
- QUANTIFICATION AND STATISTICAL ANALYSIS

RESOURCE AVAILABILITY

Lead contact

Further information and requests for resources and reagents should be directed to and will be fulfilled by the lead contact, Dr Diego Javier Jiménez (diego.jimenezavella@kaust.edu.sa).

Materials availability

This study did not generate new unique reagents.

Data and code availability

DNA sequencing data (amplicon and whole metagenome) have been deposited at European Nucleotide Archive (ENA) (BioProject ID PRJEB72453) are publicly available as of the date of publication. Accession numbers are listed in the key resources table. This paper does not report original code. Any additional information required to reanalyze the data reported in this paper is available from the lead contact upon request.

Author contributions

Author contributions following the CRediT taxonomy (<https://casrai.org/credit/>) are as follows: conceptualization: D.J.J.; data curation: D.J.J., D.C., F.S., G.C., G.F., L.D-G., L.M., Y.P.O.S.; formal analysis: D.J.J., D.C., F.S., G.C., G.F., M.C., L.D-G., L.M., Y.P.O.S., F.S.G.; funding acquisition: D.J.J., A.S.R.; investigation: D.J.J., D.C., F.S., G.C., G.F., L.D-G., L.M., Y.P.O.S., C.R-L.; methodology: D.J.J., D.C., F.S., G.C., G.F., M.C., L.D-G., L.M., Y.P.O.S., F.S.G.; project administration: D.J.J.; resources: D.J.J., F.S.G., W.S., A.R., F.D-A.; software: D.J.J., G.C., G.F., M.C., L.D-G., L.M., A.R.; supervision: D.J.J.;

validation: D.J.J., D.C., F.S., CG, G.F., L.D-G., L.M., Y.P.O.S.; visualization: D.J.J.; writing—original draft: D.J.J.; writing—review and editing: D.J.J., G.C., L.D-G., L.M., F.S.G., W.S., F.D-A., A.R., A.S.R.

Acknowledgments

We thank Ricardo Serrano from Minipack SAS company for providing the PET particles as well as Luis Miguel Rodriguez for his comments about taxa names and phylogenies. We thank Intikhab Alam for the search for the M5 motif in our putative PETases. We thank the Faculty of Sciences at the Universidad de los Andes (Colombia) for providing financial and administrative support. For sequencing, the DNA samples were exported under the ANLA exportation permit number 2784. The computational results presented here were achieved, in part, using the ExaCore—IT Core-facility at the Vice Presidency for Research and Creation at the Universidad de los Andes. This study was partially funded by the FAPA project (number PR.3.2018.5287) obtained by D.J.J. at the Department of Biological Sciences in Universidad de los Andes, and baseline resources (BAS/1/1096-01-01) were obtained from Alexandre S. Rosado at KAUST. We also thank the MENZYPOL network (<https://ms.hereon.de/menzypol/>) for providing the mobility resources under grant agreement 78978 from the Colombian Ministry of Science, Technology, and Innovation. M.C. was funded by an Australian Research Council Discovery Project (grant number DP220100900). F.D-A. was supported by the USDA National Institute of Food and Agriculture and Hatch Appropriations under Project PEN04908 and Accession number 7006279.

Declaration of interests

The authors declare no competing interests.

Supplemental information

Supplemental information to this article can be found online at <https://doi.org/10.1016/j.tibtech.2024.08.013>.

References

- Andreato, F.D. *et al.* (2012) The microbiome of Brazilian mangrove sediments as revealed by metagenomics. *PLoS ONE* 7, e38600
- Allard, S.M. *et al.* (2020) Introducing the Mangrove Microbiome Initiative: identifying microbial research priorities and approaches to better understand, protect, and rehabilitate mangrove ecosystems. *mSystems* 5, e00659–20
- Anu, K. *et al.* (2024) Mangroves in environmental engineering: Harnessing the multifunctional potential of Nature's coastal architects for sustainable ecosystem management. *Results Eng.* 21, 101765
- van Bijsterveldt, C.E.J. *et al.* (2021) Does plastic waste kill mangroves? A field experiment to assess the impact of macroplastics on mangrove growth, stress response and survival. *Sci. Total Environ.* 756, 143826
- Goldberg, L. *et al.* (2020) Global declines in human-driven mangrove loss. *Glob. Chang. Biol.* 26, 5844–5855
- Rillig, M.C. *et al.* (2019) The role of multiple global change factors in driving soil functions and microbial biodiversity. *Science* 366, 886–890
- Garcés-Ordóñez, O. *et al.* (2019) Marine litter and microplastic pollution on mangrove soils of the Ciénaga Grande de Santa Marta, Colombian Caribbean. *Mar. Pollut. Bull.* 145, 455–462
- Martin, C. *et al.* (2020) Exponential increase of plastic burial in mangrove sediments as a major plastic sink. *Sci. Adv.* 6, eaaz5593
- Deng, H. *et al.* (2021) Microplastics pollution in mangrove ecosystems: a critical review of current knowledge and future directions. *Sci. Total Environ.* 753, 142041
- Lear, G. *et al.* (2021) Plastics and the microbiome: impacts and solutions. *Environ. Microbiome* 16, 2
- Jiménez, D.J. *et al.* (2022) Merging plastics, microbes, and enzymes: highlights from an international workshop. *Appl. Environ. Microbiol.* 88, e00721–22
- Rillig, M.C. *et al.* (2023) The soil plastsphere. *Nat. Rev. Microbiol.* 22, 64–74
- Jiménez, D.J. *et al.* (2015) Compositional profile of α / β -hydrolase fold proteins in mangrove soil metagenomes: prevalence of epoxide hydrolases and haloalkane dehalogenases in oil-contaminated sites. *Microb. Biotechnol.* 8, 604–613
- Auta, H.S. *et al.* (2018) Growth kinetics and biodeterioration of polypropylene microplastics by *Bacillus* sp. and *Rhodococcus* sp. isolated from mangrove sediment. *Mar. Pollut. Bull.* 127, 15–21
- Chen, C.-C. *et al.* (2020) Enzymatic degradation of plant biomass and synthetic polymers. *Nat. Rev. Chem.* 4, 114–126
- Ren, S.Y. and Ni, H.G. (2023) Biodeterioration of microplastics by bacteria isolated from mangrove sediment. *Toxics* 11, 432
- Wang, Y. *et al.* (2023) Consequences of microplastics on global ecosystem structure and function. *Rev. Env. Contam. (formerly: Residue Reviews)* 261, 22
- Yang, G. *et al.* (2022) Multiple anthropogenic pressures eliminate the effects of soil microbial diversity on ecosystem functions in experimental microcosms. *Nat. Commun.* 13, 4260
- Sun, Y. *et al.* (2023) Plastsphere microbiome: methodology, diversity, and functionality. *iMeta* 2, e101
- Lozano, Y.M. *et al.* (2024) Microplastic fibres affect soil fungal communities depending on drought conditions with consequences for ecosystem functions. *Environ. Microbiol.* 26, e16549
- Yuan, Y. *et al.* (2023) Soil properties, microbial diversity, and changes in the functionality of saline-alkali soil are driven by microplastics. *J. Hazard. Mater.* 446, 130712
- Chamas, A. *et al.* (2020) Degradation rates of plastics in the environment. *ACS Sustain. Chem. Eng.* 8, 3494–3511
- Yoshida, S. *et al.* (2016) A bacterium that degrades and assimilates poly(ethylene terephthalate). *Science* 351, 1196–1199
- Danso, D. *et al.* (2018) New insights into the function and global distribution of polyethylene terephthalate (PET)-degrading bacteria and enzymes in marine and terrestrial metagenomes. *Appl. Environ. Microbiol.* 84, e02773–17
- Erickson, E. *et al.* (2022) Sourcing thermotolerant poly(ethylene terephthalate) hydrolase scaffolds from natural diversity. *Nat. Commun.* 13, 7850
- Qi, X. *et al.* (2023) Glacier as a source of novel polyethylene terephthalate hydrolases. *Environ. Microbiol.* 25, 2822–2833
- Khairul Anuar, N.F.S. *et al.* (2022) An overview into polyethylene terephthalate (PET) hydrolases and efforts in tailoring enzymes for improved plastic degradation. *Int. J. Mol. Sci.* 23, 12644
- Jayasekara, S.K. *et al.* (2023) Trends in in-silico guided engineering of efficient polyethylene terephthalate (PET) hydrolyzing enzymes to enable bio-recycling and upcycling of PET. *Comput. Struct. Biotechnol. J.* 21, 3513–3521

29. Arnal, G. *et al.* (2023) Assessment of four engineered PET degrading enzymes considering large-scale industrial applications. *ACS Catal.* 13, 13156–13166
30. Qi, X. *et al.* (2021) Evaluation of PET degradation using artificial microbial consortia. *Front. Microbiol.* 12, 778828
31. Roberts, C. *et al.* (2020) Environmental consortium containing *Pseudomonas* and *Bacillus* species synergistically degrades polyethylene terephthalate plastic. *mSphere* 5, 01151–20
32. Bao, T. *et al.* (2023) Engineering microbial division of labor for plastic upcycling. *Nat. Commun.* 14, 5712
33. Jiang, W. *et al.* (2023) Characterization of a novel esterase and construction of a *Rhodococcus-Burkholderia* consortium capable of catabolism bis (2-hydroxyethyl) terephthalate. *Environ. Res.* 238, 117240
34. Jiménez, D.J. *et al.* (2024) Engineering microbiomes to transform plastics. *Trends Biotechnol.* 42, 265–268
35. Salinas, J. *et al.* (2023) Development of plastic-degrading microbial consortia by induced selection in microcosms. *Front. Microbiol.* 14, 1143769
36. Zhao, S. *et al.* (2023) Biodegradation of polyethylene terephthalate (PET) by diverse marine bacteria in deep-sea sediments. *Environ. Microbiol.* 25, 2719–2731
37. Hu, H. *et al.* (2022) Guided by the principles of microbiome engineering: accomplishments and perspectives for environmental use. *mLife* 1, 382–398
38. Diaz-García, L. *et al.* (2021) Top-down enrichment strategy to cocultivate lactic acid and lignocellulolytic bacteria From the *Megathyrus maximus* phyllosphere. *Front. Microbiol.* 12, 744075
39. Sánchez, Á. *et al.* (2024) The optimization of microbial functions through rational environmental manipulations. *Mol. Microbiol.*, Published online February 19, 2024. <https://doi.org/10.1111/mmi.15236>
40. Diaz-García, L. *et al.* (2024) Andean soil-derived lignocellulolytic bacterial consortium as a source of novel taxa and putative plastic-active enzymes. *Syst. Appl. Microbiol.* 47, 126485
41. Jiménez, D.J. *et al.* (2014) Novel multispecies microbial consortia involved in lignocellulose and 5-hydroxymethylfurfural bioconversion. *Appl. Microbiol. Biotechnol.* 98, 2789–2803
42. Arias-Sánchez, F.I. *et al.* (2019) Artificially selecting microbial communities: if we can breed dogs, why not microbiomes? *PLoS Biol.* 17, e3000356
43. Rillig, M.C. *et al.* (2016) Soil microbes and community coalescence. *Pedobiologia* 59, 37–40
44. Custer, G.F. *et al.* (2024) Toward an integrative framework for microbial community coalescence. *Trends Microbiol.* 32, 241–251
45. Châtillon, E. *et al.* (2023) New insights into microbial community coalescence in the land-sea continuum. *Microbiol. Res.* 267, 127259
46. Huet, S. *et al.* (2023) Experimental community coalescence sheds light on microbial interactions in soil and restores impaired functions. *Microbiome* 11, 42
47. de Souza Machado, A.A. *et al.* (2018) Impacts of microplastics on the soil biophysical environment. *Environ. Sci. Technol.* 52, 9656–9665
48. Jacquin, J. *et al.* (2021) Microbial diversity and activity during the biodegradation in seawater of various substitutes to conventional plastic cotton swab sticks. *Front. Microbiol.* 12, 604395
49. Pinto, M. *et al.* (2022) Microbial consortiums of putative degraders of low-density polyethylene-associated compounds in the ocean. *mSystems* 7, e01415–21
50. Pinto, M. *et al.* (2020) Putative degraders of low-density polyethylene-derived compounds are ubiquitous members of plastic-associated bacterial communities in the marine environment. *Environ. Microbiol.* 22, 4779–4793
51. Castledine, M. *et al.* (2020) Community coalescence: an eco-evolutionary perspective. *Philos. Trans. R. Soc. Lond. Ser. B Biol. Sci.* 375, 20190252
52. Meyer-Cifuentes, I.E. *et al.* (2020) Synergistic biodegradation of aromatic-aliphatic copolyester plastic by a marine microbial consortium. *Nat. Commun.* 11, 5790
53. James-Pearson, L.F. *et al.* (2023) A hot topic: thermophilic plastic biodegradation. *Trends Biotechnol.* 41, 1117–1126
54. Koike, H. *et al.* (2023) *Alcanivorax* bacteria as important polypropylene degraders in mesopelagic environments. *Appl. Environ. Microbiol.* 89, e01365–23
55. Zadjelovic, V. *et al.* (2022) A mechanistic understanding of polyethylene biodegradation by the marine bacterium *Alcanivorax*. *J. Hazard. Mater.* 436, 129278
56. Kurm, V. *et al.* (2016) Low abundant soil bacteria can be metabolically versatile and fast growing. *Ecology* 98, 555–564
57. Kato, S. *et al.* (2018) Isolation of previously uncultured slow-growing bacteria by using a simple modification in the preparation of agar media. *Appl. Environ. Microbiol.* 84, e00807–18
58. Schaerer, L.G. *et al.* (2023) Versatile microbial communities rapidly assimilate ammonium hydroxide-treated plastic waste. *J. Ind. Microbiol. Biotech.* 50, kuad008
59. Schaerer, L. *et al.* (2023) Coexistence of specialist and generalist species within mixed plastic derivative-utilizing microbial communities. *Microbiome* 11, 224
60. Skariyachan, S. *et al.* (2018) Enhanced polymer degradation of polyethylene and polypropylene by novel thermophilic consortia of *Brevibacillus* sp. and *Aneurinibacillus* sp. screened from waste management landfills and sewage treatment plants. *Polym. Degrad. Stab.* 149, 52–68
61. Dimassi, S.N. *et al.* (2023) Insights into the degradation mechanism of PET and PP under marine conditions using FTIR. *J. Hazard. Mater.* 447, 130796
62. Kotova, I.B. *et al.* (2021) Microbial degradation of plastics and approaches to make it more efficient. *Microbiology* 90, 671–701
63. Sriromreun, P. *et al.* (2013) Standard methods for characterizations of structure and hydrolytic degradation of aliphatic/aromatic copolyesters. *Polym. Degrad. Stab.* 98, 169–176
64. Xia, X.I. *et al.* (2014) Degradation behaviors, thermostability and mechanical properties of poly (ethylene terephthalate)/polylactic acid blends. *J. Cent. South Univ.* 21, 1725–1732
65. Obrador-Viel, T. *et al.* (2024) Assessing microbial plastic degradation requires robust methods. *Microb. Biotechnol.* 17, e14457
66. Sander, M. *et al.* (2019) Assessing the environmental transformation of nanoplastic through ¹³C-labelled polymers. *Nat. Nanotechnol.* 14, 301–303
67. Wang, P. *et al.* (2023) Polyethylene mulching film degrading bacteria within the plastisphere: Co-culture of plastic degrading strains screened by bacterial community succession. *J. Hazard. Mater.* 442, 130045
68. Wang, X. *et al.* (2019) Biodegradation mechanism of polyesters by hydrolase from *Rhodospseudomonas palustris*: an in-silico approach. *Chemosphere* 231, 126–133
69. Meng, D. *et al.* (2021) *Mesorhizobium xinjiangense* sp. nov., isolated from rhizosphere soil of *Alhagi sparsifolia*. *Arch. Microbiol.* 204, 29
70. Tariq, A. *et al.* (2022) *Alhagi sparsifolia*: an ideal phreatophyte for combating desertification and land degradation. *Sci. Total Environ.* 844, 157228
71. Ye, Y. *et al.* (2020) *Nitratireductor mangrovi* sp. nov., a nitrate-reducing bacterium isolated from mangrove soil. *Curr. Microbiol.* 77, 1334–1340
72. Pan, X.C. *et al.* (2014) *Nitratireductor shengliensis* sp. nov., isolated from an oil-polluted saline soil. *Curr. Microbiol.* 69, 561–566
73. Marasco, R. *et al.* (2023) The identification of the new species *Nitratireductor thuwali* sp. nov. reveals the untapped diversity of hydrocarbon-degrading culturable bacteria from the arid mangrove sediments of the Red Sea. *Front. Microbiol.* 14, 1155381
74. Hedlund, B.P. *et al.* (2022) SeqCode: a nomenclatural code for prokaryotes described from sequence data. *Nat. Microbiol.* 7, 1702–1708
75. Sasoh, M. *et al.* (2006) Characterization of the terephthalate degradation genes of *Comamonas* sp. strain E6. *Appl. Environ. Microbiol.* 72, 1825–1832
76. Putman, L.I. *et al.* (2023) Deconstructed plastic substrate preferences of microbial populations from the natural environment. *Microbiol. Spectr.* 11, e0036223
77. Buchholz, P.C.F. *et al.* (2022) Plastics degradation by hydrolytic enzymes: The plastics-active enzymes database—PAZy. *Proteins* 90, 1443–1456
78. Alam, I. *et al.* (2020) Rapid evolution of plastic-degrading enzymes prevalent in the global ocean. *bioRxiv*, Published online September 9, 2020. <https://doi.org/10.1101/2020.09.07.285692>
79. Maruthamuthu, M. *et al.* (2017) Characterization of a furan aldehyde-tolerant β -xylosidase/ α -arabinosidase obtained through a synthetic metagenomics approach. *J. Appl. Microbiol.* 123, 145–158

80. Callahan, B.J. *et al.* (2016) DADA2: High-resolution sample inference from Illumina amplicon data. *Nat. Methods* 13, 581–583
81. Martin, M. (2011) Cutadapt removes adapter sequences from high-throughput sequencing reads. *EMBnet J.* 17, 10–12
82. Kursu, M.B. and Rudnicki, W.R. (2010) Feature selection with the Boruta package. *J. Stat. Softw.* 36, 1–13
83. Love, M.I. *et al.* (2014) Moderated estimation of fold change and dispersion for RNA-seq data with DESeq2. *Genome Biol.* 15, 550
84. Friedman, J. and Alm, E.J. (2012) Inferring correlation networks from genomic survey data. *PLoS Comput. Biol.* 8, e1002687
85. Bastian, M. *et al.* (2009) Gephi: an open source software for exploring and manipulating networks. *Proc. Int. AAAI Conf. Weblogs. Soc. Media* 3, 361–362
86. Diaz-García, L. *et al.* (2021) Dilution-to-stimulation/extinction method: a combination enrichment strategy to develop a minimal and versatile lignocellulolytic bacterial consortium. *Appl. Environ. Microbiol.* 87, e02427–20
87. Bolyen, E. *et al.* (2019) Reproducible, interactive, scalable and extensible microbiome data science using QIIME 2. *Nat. Biotechnol.* 37, 852–857
88. Yilmaz, P. *et al.* (2014) The SILVA and ‘All-species Living Tree Project (LTP)’ taxonomic frameworks. *Nucleic Acids Res.* 42, D643–D648
89. Lessa Belone, M.C. *et al.* (2021) Degradation of common polymers in sewage sludge purification process developed for microplastic analysis. *Environ. Pollut.* 269, 116235
90. Menzel, P. *et al.* (2016) Fast and sensitive taxonomic classification for metagenomics with Kaiju. *Nat. Commun.* 7, 11257
91. Li, D. *et al.* (2015) MEGAHIT: an ultra-fast single-node solution for large and complex metagenomics assembly via succinct de Bruijn graph. *Bioinformatics* 31, 1674–1676
92. Alneberg, J. *et al.* (2014) Binning metagenomic contigs by coverage and composition. *Nat. Methods* 11, 1144–1146
93. Kang, D.D. *et al.* (2019) MetaBAT 2: an adaptive binning algorithm for robust and efficient genome reconstruction from metagenome assemblies. *PeerJ* 7, e7359
94. Wu, Y.-W. *et al.* (2016) MaxBin 2.0: an automated binning algorithm to recover genomes from multiple metagenomic datasets. *Bioinformatics* 32, 605–607
95. Sieber, C.M.K. *et al.* (2018) Recovery of genomes from metagenomes via a dereplication, aggregation and scoring strategy. *Nat. Microbiol.* 3, 836–843
96. Parks, D.H. *et al.* (2015) CheckM: assessing the quality of microbial genomes recovered from isolates, single cells, and metagenomes. *Genome Res.* 25, 1043–1055
97. Tanizawa, Y. *et al.* (2018) DFAST: a flexible prokaryotic genome annotation pipeline for faster genome publication. *Bioinformatics* 34, 1037–1039
98. Langmead, B. and Salzberg, S.L. (2012) Fast gapped-read alignment with Bowtie 2. *Nat. Methods* 9, 357–359
99. Danecek, P. *et al.* (2021) Twelve years of SAMtools and BCFtools. *Gigascience* 10, giab008
100. Chaumeil, P.-A. *et al.* (2022) GTDB-Tk v2: memory friendly classification with the genome taxonomy database. *Bioinformatics* 38, 5315–5316
101. Rodriguez-R, L.M. *et al.* (2018) The Microbial Genomes Atlas (MiGA) webserver: taxonomic and gene diversity analysis of Archaea and Bacteria at the whole genome level. *Nucleic Acids Res.* 46, W282–W288
102. Meier-Kolthoff, J. and Göker, M. (2019) TYGS is an automated high-throughput platform for state-of-the-art genome-based taxonomy. *Nat. Commun.* 10, 2182
103. Meier-Kolthoff, J. *et al.* (2013) Genome sequence-based species delimitation with confidence intervals and improved distance functions. *BMC Bioinforma.* 14, 60
104. Nguyen, L.T. *et al.* (2015) IQ-TREE: a fast and effective stochastic algorithm for estimating maximum-likelihood phylogenies. *Mol. Biol. Evol.* 32, 268–274
105. Letunic, I. and Bork, P. (2021) Interactive Tree Of Life (ITOL) v5: an online tool for phylogenetic tree display and annotation. *Nucleic Acids Res.* 49, W293–W296
106. Fu, L. *et al.* (2012) CD-HIT: accelerated for clustering the next-generation sequencing data. *Bioinformatics* 28, 3150–3152
107. Buchfink, B. *et al.* (2015) Fast and sensitive protein alignment using DIAMOND. *Nat. Methods* 12, 59–60
108. Aramaki, T. *et al.* (2020) KofamKOALA: KEGG Ortholog assignment based on profile HMM and adaptive score threshold. *Bioinformatics* 36, 2251–2252
109. Sulaiman, S. *et al.* (2012) Isolation of a novel cutinase homolog with polyethylene terephthalate-degrading activity from leaf-branch compost by using a metagenomic approach. *Appl. Environ. Microbiol.* 78, 1556–1562
110. Furukawa, M. *et al.* (2019) Efficient degradation of poly(ethylene terephthalate) with *Thermobifida fusca* cutinase exhibiting improved catalytic activity generated using mutagenesis and additive-based approaches. *Sci. Rep.* 9, 16038
111. Zallot, R. *et al.* (2019) The EFI web resource for genomic enzymology tools: leveraging protein, genome, and metagenome databases to discover novel enzymes and metabolic pathways. *Biochemistry* 58, 4169–4182
112. Shannon, P. *et al.* (2003) Cytoscape: a software environment for integrated models of biomolecular interaction networks. *Genome Res.* 13, 2498–2504
113. Anderson, M.J. and Walsh, D.C.I. (2013) PERMANOVA, ANOSIM, and the Mantel test in the face of heterogeneous dispersions: what null hypothesis are you testing? *Ecol. Monogr.* 83, 557–574
114. Wickham, H. (2016) *ggplot2: Elegant Graphics for Data Analysis*, Springer-Verlag

STAR★METHODS

KEY RESOURCES TABLE

Reagent or resource	Source	Identifier
Chemicals, peptides, and recombinant proteins		
Dibasic sodium phosphate [Na ₂ HPO ₄]	Sigma-Aldrich	Cat# 7558-79-4
Dibasic potassium phosphate [K ₂ HPO ₄]	Sigma-Aldrich	Cat# 7758-11-4
Ammonium sulfate [(NH ₄) ₂ SO ₄]	Sigma-Aldrich	Cat# 7783-20-2
Calcium nitrate hydrate [Ca(NO ₃) ₂]	Sigma-Aldrich	Cat# 35054-52-5
Magnesium chloride [MgCl ₂]	Sigma-Aldrich	Cat# 7786-30-3
Critical commercial assays		
DNeasy PowerSoil Kit	Qiagen	Cat# 47014
DNeasy UltraClean microbial kit	Qiagen	Cat# 12224-50
Deposited data		
Raw data files for DNA sequencing	This paper	European Nucleotide Archive (ENA) (BioProject ID PRJEB72453)
Oligonucleotides		
Primers for 16S rRNA amplification (primers Bakt_341F and Bakt_805R)	Macrogen, Inc.	N/A
Primers for ITS2 amplification (primers ITS3 and ITS4)	Macrogen, Inc.	N/A
Software and algorithms		
DADA2	Open source	https://benjjneb.github.io/dada2/tutorial.html
Phyloseq	Open source	https://joey711.github.io/phyloseq/
QIIME2	Open source	https://qiime2.org
DESeq2	Open source	https://bioconductor.org/packages/release/bioc/html/DESeq2.html
Boruta	Open source	https://gitlab.com/mbq/Boruta/
SparCC	Open source	https://github.com/bio-developer/sparcc
MEGAHIT	Open source	https://github.com/voutcn/megahit
CheckM	Open source	https://github.com/ECogenomics/CheckM
GTDBTk	Open source	https://github.com/ECogenomics/GTDBTk
MiGA	Open source	https://github.com/bio-miga/miga
HMMER	Open source	https://github.com/EddyRivasLab/hmmer
KofamKOALA	Open source	https://github.com/takaram/kofam_scan
Enzyme Similarity Tool	Open source	https://efi.igb.illinois.edu/efi-est/
Other		
PET particles	Eastar TM Copolyester GN071	https://www.eastman.com/en/products/product-detail/71015643/eastar-gn071-copolyester-natural
Nicolet iS50 FTIR Spectrometer	Thermo Scientific	N/A
SDT Q600 Thermal Analyzer	TA Instruments	N/A
Q2000 differential scanning calorimeter	TA Instruments	N/A

METHOD DETAILS

Setup of soil microcosm experiments

We used a laboratory-based microcosm approach to evaluate the effects of PET particle input on the mangrove soil microbiome in the presence or absence of seawater. First, 25 soil samples (~500 g each) were collected from Barú peninsula (Cartagena de Indias,

Colombia; 10°15'48.5"N, 75°35'29.8"W). Soil sampling was performed under Autoridad Nacional de Licencias Ambientales (ANLA) permit number 2021123746-1-000. At the time of sampling, macroplastic items were observed on the mangrove soil surface. Fresh soil samples were homogenized and passed through a 2-mm metal sieve. The obtained soil was then used to set up individual microcosms in 100-mL Erlenmeyer flasks. The experimental design consisted of four treatments (soil, soil + seawater, soil + PET particles (dimension < 5 mm), and soil + seawater + PET particles), with four replicates sampled at two timepoints (see Figure 1A in the main text). Depending on the treatment, the microcosms contained 15 g of soil, 15 mL of seawater, and 1.5 g of semicrystalline PET particles (final concentration: 10% w/w). PET particles (Eastar TM Copolyester GN071) were obtained from MiniPack SAS (Bogotá, Colombia) (<https://www.minipak.com.co/>). The soil microcosms were incubated at 30°C for 30 or 90 days (two sampling points). During the experiment, a desiccation gradient was observed due to the status of seawater inclusion and time of incubation (Figure 1A). After 30 and 90 days of incubation, plastic particles were manually removed from the microcosm, and the remaining soil was collected for DNA extraction using DNeasy PowerSoil Kit (Qiagen, Maryland, USA), as per the manufacturer's instructions.

Microbial diversity analyses from the microcosms

High-quality microbial DNA from soils was sent to Macrogen, Inc. (Seoul, Korea) for bacterial 16S rRNA gene amplicon sequencing of the V3–V4 region (primers Bakt_341F and Bakt_805R) and internal transcribed spacer (ITS) 2 region (primers ITS3 and ITS4) using the Illumina MiSeq platform (300bp paired-end reads). Raw sequences were processed using DADA2 pipeline [80]. Briefly, the primers were removed using Cutadapt [81]. Then, sequences were filtered and trimmed, errors were identified and corrected, and paired sequences were merged and dereplicated before assigning taxonomy to bacteria and fungi using SILVA rRNA gene database (v.138) and UNITE database (v.10.5.2021), respectively. The processed reads were then imported to phyloseq, and nonfungal and nonbacterial reads were removed based on their taxonomic assignments. ASV tables were rarefied to 10 000 or 5000 reads in the 16S rRNA gene and ITS2 region, respectively, for downstream analysis including comparisons of diversity metrics (alpha and beta) and statistical analysis (e.g., PERMANOVA). The Boruta algorithm [82] and DESeq2 [83] were also used to analyze these sequencing data (see quantification and statistical analysis section). Nonrandom co-occurrence analyses were performed using SparCC [84]. For this purpose, we selected the ASVs with a minimum of 30 sequences, accounting for >90% of the sequences. For each network, *p*-values were obtained based on 99 permutations of random selections of the data table. SparCC correlations with a magnitude >0.7 or <−0.7 and statistical significance (*p* < 0.01) were included in network analyses. Nodes within the reconstructed networks represented ASVs, whereas edges represented strong and significant correlations between nodes. Network topology was assessed using various metrics, including node and edge counts, modularity, community numbers, average path length, network diameter, averaged degree, and clustering coefficient. Network visualization and properties were constructed using Gephi v0.1 software [85].

Artificial selection strategy

We used the top–down strategy of dilution-to-stimulation to select PET-transforming microbial consortia from a mangrove soil microcosm. For this, a randomly selected microcosm containing soil, PET particles, and seawater (after 90 days of incubation) was used as a microbial source. The microbial inoculum was prepared by adding 10 g of sampled mangrove soil and 10 g of sterile glass beads to 90 ml of mineral salt medium (MSM) (7 g/liter Na₂HPO₄, 2 g/liter K₂HPO₄, 1 g/liter (NH₄)₂SO₄, 0.1 g/liter Ca(NO₃)₂, 0.2 g/liter MgCl₂, pH 7.5) in an Erlenmeyer flask. The flask was shaken for 20 min at 250 rpm [86]. Then, 250 μL of the soil suspension was added to 100-mL Erlenmeyer flasks in triplicate. Each flask comprised 25 mL of mineral salt medium (MSM) containing 1% PET particles supplemented with 25 μL of a trace element solution (2.5 g/liter EDTA, 1.5 g/liter FeSO₄, 0.025 g/liter CoCl₂, 0.025 g/liter ZnSO₄, 0.015 g/liter MnCl₂, 0.015 g/liter NaMoO₄, 0.01 g/liter NiCl₂, 0.02 g/liter H₃BO₃, 0.005 g/liter CuCl₂) and 25 μL of a vitamin solution (0.1 g/liter Ca-panthothenate, 0.1 g/liter cyanocobalamine, 0.1 g/liter nicotinic acid, 0.1 g/liter pyridoxal, 0.1 g/liter riboflavin, 0.1 g/liter thiamin, 0.01 g/liter biotin, 0.1 g/liter folic acid) [41] (see Figure 1B in the main text). PET beads were washed twice with distilled water and 70% (v/v) ethanol and then air-dried in an oven at 50°C for 12 h. Subsequently, the plastic beads were knife-milled through a 1-mm screen under aseptic conditions. For transfer 1 (T1), the Erlenmeyer flask cultures were incubated under aerobic conditions (130 rpm) at 30°C for 27 days (see Figure 1B in the main text). Then, culture conditions were modified. For T2, we added 2.5 mg of peptone to MSM, whereas no peptone was added for T3. From T3 to T6, 250-μL aliquots of the microbial suspension were used as the inoculum for the next transfer. From T4, the microbial seed for subsequent growth cycles was obtained from replicate 3 (R3) after T3, and eight biological replicates were set up and incubated at 40°C for 14 days. For T5, the incubation time was increased to 56 days. Two controls (i.e., without substrate or microbial source) were also set up and subjected to the same conditions. At the end of each batch culture, the flasks were gently shaken, PET particles were allowed to settle, and the liquid fraction was removed by pipetting to determine OD₆₀₀.

Bacterial diversity during enrichment cultures

As microbial growth was extremely limited during the enrichment process, the total volume of each replicate flask (25 mL) was centrifuged, and the cell pellet was resuspended in 2 mL of MSM. Then, DNA was extracted using DNeasy UltraClean microbial kit (Qiagen, Maryland, USA) according to manufacturer's instructions. The V3–V4 region of the bacterial 16S rRNA gene was sequenced using the Illumina MiSeq platform (300bp paired-end reads) at Macrogen Inc. (Seoul, Korea) using the same primers as mentioned previously. Then, the raw sequencing data were processed using QIIME2 software [87] and DADA2 pipeline [80]. ASV taxonomic assignment was performed using the pipeline q2-feature-classifier in QIIME2 and SILVA rRNA v.138 database [87,88]. QIIME2 was also used to determine the relative abundances of ASVs, alpha and beta diversity metrics (including Shannon index), observed ASVs, and weighted UniFrac distances.

Assessments of PET structural changes

Three experimental techniques were used to gain insight into the effects of microbial growth on PET structure. In particular, we assessed the best-performing consortia (based on OD_{600}) obtained in T6 (R4T6 and R8T6). As a control, untreated PET (PET_0) and PET included in a cell-free culture medium (PET_C) were used. First, FTIR (Nicolet iS50 FTIR Spectrometer, Thermo Scientific) was performed to detect possible variations in the functional groups along the polymeric chain [61] by analyzing the absorbance spectra data between 4000 and 400 cm^{-1} using a total of 64 scans per sample at a resolution of 4 cm^{-1} . The ratio of the absorbance peak in the 1715 cm^{-1} band to the peak at 1505 cm^{-1} (taken as the reference peak) was calculated to determine the carbonyl index [89]. Then, two thermal analysis techniques, namely TGA and DSC, were performed to characterize the thermal transitions and thermal stability of the samples. TGA detects temperature variations associated with weight changes to provide insights into the occurrence of polymeric chain transformation, while DSC detects shifts in glass transition temperatures [63,64]. The TGA experiments were run in an SDT Q600 Thermal Analyzer (TA Instruments) using alumina pans and a heating ramp of 10°C/min between 30°C and 450°C under a nitrogen environment. DSC was performed in a Q2000 differential scanning calorimeter (TA Instruments) using standard aluminum pans and a heating ramp of 10°C/min between 25°C and 300°C under a nitrogen environment.

Assembly of metagenomes

Total genomic DNA extracted from the R4T6 and R8T6 bacterial consortia was used for whole-metagenome sequencing on an Illumina MiSeq platform (300bp paired-end reads). To determine a general taxonomy profile, the raw FastQ files were uploaded to the Kaiju server [90]. For the assembly, the raw sequence data (FastQ files) were initially trimmed using Sickle tool v1.33 with default parameters (accessible at <https://github.com/najoshi/sickle>). To avoid misleading results from the subsequent binning analysis, carp artifacts were detected by filtering trimmed sequences against adapter and nonauthentic primer sequences originating from the Illumina library preparation. Metagenome assembly was performed using MEGAHIT v1.2.9 [91] with default parameters. For binning, Concoct v1.1.0 [92], MetaBAT v2.12.1 [93], and MaxBin v2.2.6 [94] were used with default parameters. The binned contigs were subsequently analyzed using DAS Tool v1.1.6 [95]. To assess the completeness and contamination of the resulting bins, CheckM v1.2.2 was used with the lineage_wf option [96]. The resulting MAGs were structurally annotated and curated based on rRNAs (e.g., 5S, 16S, and 23S) and *rpoB* using DFAST v1.2.18 [97]. The percentage of mapped reads from each MAG against raw sequencing data was calculated using Bowtie v2.3.5 [98] and summarized using SAMtools v1.9 [99].

Taxonomic and phylogenetic analysis of MAGs

Taxonomic assignment of MAGs was performed using GTDB-Tk v2.3.2. [100] and GTDB database release 08-RSR214. MiGA v1.2.60 [101] was used to determine genome distance metrics based on AAI and ANI against the NCBI Prok and TypeMat databases. Other genomic features, including length, G+C content, protein counts, coding density, and 16S rRNA genes, were obtained by MiGA. The high-quality (i.e., completeness $\geq 90\%$ and contamination $\leq 5\%$) MAGs were uploaded to the Type (Strain) Genome Server (TYGS) [102] to determine dDDH values. Phylogenomic analysis based on genome sequences were carried out using GBDP method via the TYGS [103]. Additionally, phylogenetic trees, including representative genomes from the type strains, nontype strains and MAGs of the members of the *Rhizobiaceae* and *Kaistiaceae* families as defined in GTDB release 08-RSR214, were inferred using 120 single-copy protein markers via GTDB-Tk v2.3.2 and IQ-TREE v.2.1.2 [104]. Briefly, the starting trees were initially calculated using FastTree v.2.1.10 and then used to infer final trees with the mixture models as '-m LG+C10+F+G' in IQ-TREE v.2.1.2. The trees were rooted with outgroups, pruned, and beautified for illustration purposes using the Interactive Tree of Life (iTOL) online tool [105].

Detection of putative plastic-active enzymes

Putative PETases over MAGs were searched using the PAZy database [77], according to published protocols [24,40]. Briefly, the HMM was built by clustering sequences of previously published PETases from PAZy using CD-HIT [106] at a sequence identity cutoff of 90%, and the searches were performed using HMMER v3.3.2 software (<http://hmmer.org>) at an e-value cutoff of $1e^{-10}$ for putative PETases. The aligned HMM hits were subsequently blasted against the nonredundant NCBI protein database using DIAMOND v0.9 [107]. Proteins with HMM scores >70 were selected, and BLASTp was used for comparison against the PETase from *I. sakaiensis* to identify the large M5 motif [78]. We also performed functional annotation based on the KEGG ortholog assignment using the KofamKOALA Web server (<https://www.genome.jp/tools/kofamkoala/>) [108]. For this, fasta files containing the predicted proteomes per MAG were obtained from MiGA and then uploaded to the KofamKOALA Web server using default parameters. Genes with HMM bit scores >100 were retained and analyzed. To explore the metabolic potential to transform PET, we selected two KOs (K21104 and K21105) that are affiliated with enzymes involved in PET depolymerization, as well as 2 and 11 KOs related to enzymes involved in TPA and EG catabolism, respectively.

Analysis of putative plastic-active enzymes

For phylogeny reconstruction, we used 37 active PETases obtained by Erickson and colleagues [25] and five other confirmed plastic-active enzymes, namely GlacPETase [26], LCC (leaf-branch compost cutinase) [109], TfuscaCut2 [110], IsPETase, and IsMHETase [23]. Phylogenetic analysis was performed using MEGA v.11 software, according to the parameters described by Ericksson and colleagues [25]. Briefly, protein sequences were aligned using ClustalW, and the evolutionary history was inferred using the minimum evolution (ME) method. Distances (in units of the number of amino acid substitutions per site) were computed using the Jones–Taylor–Thornton matrix-based model. The ME tree was searched using the close-neighbor-interchange algorithm at a search level of 1. The neighbor-joining algorithm was used to generate the initial tree. All ambiguous positions were removed for each sequence pair using pairwise deletion. The phylogenetic trees were visualized using iTOL online tool [105]. The Enzyme Function Initiative–Enzyme Similarity Tool [111] was used to perform a BLASTall pairwise search of the amino acid sequences of PETases 1–9, MHETases 1 and 2, and 42 identified PET-active hydrolases, and the SSN was constructed with an *E*-value threshold of $1e^{-10}$ and identity of 35% (i.e., nodes representing sequences that share >35% sequence identity were connected by edges, defining SSN clusters). The SSN was visualized using Cytoscape [112].

QUANTIFICATION AND STATISTICAL ANALYSIS

The normality of residual error for alpha diversity analysis was confirmed following ANOVA. Prior to PERMANOVA testing, we assessed multivariate homogeneity using the betadispr function in the vegan package (<https://CRAN.R-project.org/package=vegan>). Although we found statistically significant deviations for homogenous variance, our balanced sampling design promotes statistically robust results [113]. For statistical analyses, bacterial and fungal amplicon datasets each contained 36 independent soil samples. We report statistical significance for amplicon sequence analysis at $\alpha = 0.05$. Next, the Boruta algorithm [82] was used to detect the features (i.e., ASVs) that explained variations between the treatment groups. Briefly, bacterial ASVs indicative of treatment groups were modeled independently using random forest analysis with 1,000 trees followed by feature selection using the Boruta algorithm. The abundance of significant ASVs (e.g., importance > 2) was z-score transformed and visualized with heat maps built using ggplot2 [114]. Finally, a differential abundance analysis was performed using DESeq2 [83] to identify differentially abundant ASVs across the treatment groups. Here, differential abundance analysis was performed parametrically using the Wald test. The statistical significance of differentially abundant taxa was determined at $\alpha = 0.05$ after FDR multiple comparisons corrections.